OFFICE OF NAVAL RESEARCH

Grant N00014-90-J-1971

R&T Code 4131pc1

Technical Report No. 12

High Resolution Infrared Spectroscopy of Pyrazine and Naphthalene in a Molecular Beam

by

Kevin B. Hewett, Meihua Shen, Christopher L. Brummel, and Laura A. Philips

Cornell University
Department of Chemistry
Ithaca, NY 14853-1301

Prepared for Publication
in the
Journal of Chemical Physics

October 26, 1993

HIGH RESOLUTION INFRARED SPECTROSCOPY OF PYRAZINE AND NAPHTHALENE IN A MOLECULAR BEAM

Kevin B. Hewett, Meihua Shen, Christopher L. Brummel and Laura A. Philips, Department of Chemistry, Cornell University, Ithaca, New York, 14853-1301.

Abstract

The high resolution infrared spectrum of pyrazine and naphthalene were measured in a molecular beam in the vicinity of the C-H stretching transition. The rotational structure in the spectrum of pyrazine from 3065-3073 cm^{-1} reveals that the C-H stretch is coupled to one other vibrational mode in the molecule. The mode coupling is manifested in the spectrum as two overlapping vibrational bands. Each of these two bands are well modeled by an asymmetric top/rigid rotor Hamiltonian. The lack of any angular momentum dependence on the coupling indicates that the vibrations are coupled by an anharmonic mechanism. The magnitude of the coupling matrix element was determined to be 0.36 cm^{-1}. The rotational structure in the spectrum of naphthalene from 3063-3067 cm^{-1} reveals that except for several local perturbations, the spectrum is well modeled by an asymmetric top/rigid rotor Hamiltonian. The local perturbations include transitions that are split into doublets as well as transitions that have been shifted from their expected positions. The magnitude of the average coupling matrix element for the doublets was determined to be 0.0016 cm^{-1}. A comparison between the vibrational mode coupling in pyrazine and naphthalene indicates that mode coupling does not correlate with the density of states in the two molecules.

I. Introduction

High resolution infrared spectroscopy has become a powerful probe of intramolecular vibrational mode coupling in the ground electronic state of small to mid-sized organic molecules[1-19]. The mechanism and/or the magnitude of mode coupling have been determined for a number of molecules including formamide[1], substituted ethanes[4-9] and a host of molecules containing acetylenic C-H stretches[11-17]. As the number and variety of molecules studied has increased, attempts have been made to correlate different physical and structural properties with the extent of vibrational mode coupling. These correlations have been made in order to

develop models of vibrational mode coupling that can then be used to predict *a priori* the nature of vibrational mode coupling in a given molecule.

Two different kinds of models have been used to predict the extent of mode coupling in different molecules. The first approach is based on the density of dark states present in the region of spectroscopic interest. This model predicts that mode coupling will become more extensive as the state density increases. The second approach is based on the underlying molecular structure of the molecules. Several different aspects of molecular structure have been suggested to play a role in vibrational mode coupling. For example, Parmenter and co-workers suggested that the low frequency, large amplitude motion of the methyl group enhanced intramolecular vibrational energy redistribution (IVR) in the electronic excited state of *p*-fluorotoluene as compared to difluorobenzene[20,21]. Another application of this approach was used by Bethardy and co-workers who analyzed available experimental data to show that molecules possessing "centers of flexibility" have faster IVR lifetimes than rigid molecules[22]. Previous work in our laboratory on both substituted ethanes and cyclobutane, suggest that both large amplitude, low frequency modes and intramolecular interactions enhance vibrational mode coupling.[5-10,23].

The two molecules considered in this study, pyrazine and naphthalene, do not possess the low frequency torsional motions that have been identified as enhancing mode coupling, but they do possess state densities that differ by nearly two orders of magnitude in the C-H stretching region. Thus, determining the vibrational mode coupling present in molecules with greatly different state densities will give some insights into the relative importance of molecular structure as compared to state densities in determining the extent of vibrational mode coupling.

The structural and spectroscopic properties of pyrazine and naphthalene are strikingly similar. Numerous experimental studies have investigated the ground state geometry of pyrazine including infrared[24-28] and Raman[25-30] spectroscopies, electron diffraction[31,32], x-ray diffraction[33], and liquid crystal NMR[32]. Naphthalene has also been investigated by a variety of experimental techniques including infrared[34-46] and Raman[38-41] spectroscopies, and x-ray diffraction[47,48]. These studies have shown that both molecules have planar structures consisting of aromatic rings, as shown in Figure 1, and both belong to the same symmetry group D_{2h}. Previous studies have also determined that in the ground electronic state the frequencies of analogous vibrational modes are similar as shown in Table I. The lowest frequency mode in pyrazine has been assigned as an out-of-plane ring deformation located at 350 cm^{-1}. Naphthalene's lowest frequency mode is the out-of-plane wing-wagging mode at 176 cm^{-1} and its second lowest mode is the out-of-plane ring deformation mode at 188 cm^{-1}. These frequencies for naphthalene are similar to the torsional frequencies found in substituted ethanes such as 2-fluoroethanol, 1,2-difluoroethane and 1-Chloro-2-fluoroethane. The structure and vibrational modes of pyrazine result in a state density that is smaller than the state density found in the substituted ethanes. Naphthalene, on the other hand has a larger state density than the substituted ethanes, not only because of its two low-frequency modes, but also because it is significantly larger than the substituted ethanes.

Extensive work has also been performed on the electronic excited states of pyrazine and naphthalene. The lowest electronic excitation of pyrazine is the $^1B_{3u} \leftarrow {}^1A_g$ transition whose origin is located at 30,876 cm^{-1}.[49-68] The fluorescence quantum yield of the origin of this transition is 0.0028,[57-67] indicating that non-radiative processes are the dominant relaxation channels

in the electronically excited molecule. In the case of pyrazine, the intersystem crossing between the $^1B_{3u}$ singlet and the $^3B_{3u}$ triplet state[57-65] has been shown to be the dominant relaxation channel. Similar work has been done on naphthalene where the two lowest electronic excitations are the $^1B_{3u} \leftarrow ^1A_g$ transition whose origin is located at 32,018 cm^{-1} and the $^1B_{2u} \leftarrow ^1A_g$ whose origin is located about 3500 cm^{-1} higher in energy[69-81]. It has been shown that extensive vibronic coupling occurs between these two electronic states[75-78], complicating the energy relaxation picture. The fluorescence quantum yield of naphthalene at the origin of the lowest singlet transition is 0.45,[71-74] indicating that non-radiative processes compete with fluorescence as relaxation channels. At low excitation energies, intersystem crossing between the $^1B_{3u}$ singlet and the triplet state $^3B_{3u}$ is the preferred non-radiative channel[72]. As the excitation energy increases, internal conversion to the ground state becomes important, until at high energy it is the preferred non-radiative channel[72]. These previous studies on pyrazine and naphthalene have clearly demonstrated that in the electronic excited state, energy redistribution occurs by a variety of pathways, and that the nature of specific rotational and vibrational levels plays an important role.

In this study we examine the vibrational mode coupling present in both pyrazine and naphthalene on the ground state potential surface using high resolution infrared spectroscopy in a molecular beam. The spectrum of one of the C-H stretching modes, located near 3065 cm^{-1}, is measured for each molecule. The significance of mode coupling in these two molecules is related to molecular structure and to the density of states.

II. Experimental

The spectra of pyrazine and naphthalene were collected using two similar experimental setups. The first setup was the high resolution infrared, optothermal spectrometer described in detail elsewhere[5,6]. This apparatus was used to collect the spectrum of pyrazine. The second setup was a modification of the first and was used to collect the spectrum of naphthalene. The experimental apparatus used in both experiments will be described briefly here and the modifications highlighted.

Pyrazine

The high resolution infrared laser beam is generated by a color-center laser (Burleigh FCL-20) which is pumped by an argon ion (Coherent Innova 15) pumped dye laser (Coherent 599). This laser system produces 3-5 mW of tunable infrared radiation with a spectral resolution of 7 MHz. In order to collect the spectrum of pyrazine the laser was scanned over the spectral region 3065-3073 cm^{-1} which corresponds to the frequency of the highest energy, infrared active C-H stretching mode, ν_{15}, as shown in Table I. The laser was continuously monitored by a 750 MHz etalon, a 7.5 GHz spectrum analyzer and a PbSe power detector. These instruments were used for the detection and correction of non-linearities in the frequency scan and laser power fluctuations as described elsewhere[5,6]. In addition to the laser power fluctuations, the intensities of the peaks were also corrected for desensitization of the bolometer over time. The laser was mechanically chopped at 250 Hz for phase sensitive detection using a lock-in amplifier. The laser was focused onto the molecular beam and multipassed approximately 40 times using two parallel mirrors. Multipassing decreased the spectral resolution to 12 MHz, but increased the signal to noise ratio by a factor of

eight. The signal to noise ratio, as measured on an acetylene ν_3 transition located at 3297.1857 cm^{-1}, was 10,000 to 1. For pyrazine, the typical signal to noise ratio was 30 to 1 due to the smaller absorption cross section.

The molecular beam was created by expanding a mixture of helium and pyrazine through a 50 μm pinhole into the first of three differentially pumped vacuum chambers. The resulting free jet was skimmed by a 1.1 mm skimmer located approximately 4 cm from the expansion nozzle. The beam continued into the second chamber where the laser beam crossed the molecular beam. An 8 mm aperture separated this second chamber from the third chamber which housed the bolometer detector. The bolometer consisted of a gallium doped silicon surface with a 2 mm by 6 mm diamond mounted on it to increase the surface area. A 2 mm aperture was mounted in front of the diamond surface. The bolometer was cooled to approximately 1.6 K using liquid helium. The signal from the bolometer was sent to the lock-in amplifier.

Pyrazine (99%+) was purchased from Aldrich Chemical Company and was used without further purification. Pyrazine was seeded into the molecular beam by passing helium through a stainless steel reservoir located immediately behind the nozzle. The pyrazine was ground into a fine powder and supported on cotton in the reservoir. The sample reservoir was either maintained at room temperature or heated to 65 °C, to achieve sufficient amounts of sample in the beam. Expansion was achieved with a backing pressure of 30-50 psig. These expansion conditions resulted in a rotational temperature of 3 K.

Naphthalene

The same laser system was used to collect the spectrum of naphthalene except that a new RbCl:Li crystal was installed in the FCL-20 laser. The new crystal increased the output power from the laser, giving 12-18 mW of tunable infrared radiation in the spectral region 3062-3068 cm^{-1}. This region corresponds to the frequency of the highest energy infrared active C-H stretching mode, ν_{29}, as shown in Table I. The same diagnostics were used to linearize and correct for the power fluctuations and bolometer desensitization. The laser was mechanically chopped at 250 Hz and then focused onto the molecular beam and multipassed approximately 10 times by two parallel mirrors.

The molecular beam system was modified in order to collect the naphthalene spectrum. The molecular beam was created by expanding a mixture of helium and naphthalene through a 50 μm pinhole into the first of two differentially pumped vacuum chambers. The resulting free jet was crossed by the laser beam before passing through a 1.1 mm skimmer into the second chamber which housed the bolometer detector. The bolometer was located approximately 25 cm from the nozzle. The modifications of the laser and molecular beam systems resulted in a factor of three increase in the signal to noise ratio over the apparatus used to collect the pyrazine spectrum. The signal to noise ratio, as measured on an acetylene ν_3 transition located at 3297.1857 cm^{-1}, was 30,000 to 1. For naphthalene, the typical signal to noise ratio was 8 to 1 due to the smaller absorption cross section.

Naphthalene was purchased from Fischer Scientific and was used without further purification. Naphthalene was seeded into the molecular beam by passing helium through a stainless steel reservoir immediately behind the nozzle. The naphthalene was ground into a fine powder and

supported on cotton in the reservoir. The sample reservoir was heated to either 100 °C or to 120 °C. The lower temperature was used with a backing pressure of 20 psig resulting in a rotational temperature of 9 K. The higher temperature was used with a backing pressure of 60 psig resulting in a rotational temperature of 5 K.

III. Results

The high resolution infrared spectra of pyrazine and naphthalene in the C-H stretching region are shown in Figure 2A and 3A respectively. The individual rotational transitions in each spectrum were assigned quantum numbers by comparing a calculated spectrum with each experimental spectrum. To calculate the spectrum, several parameters were needed including the three ground state rotational constants, three excited state rotational constants, the orientation of the transition dipole with respect to the inertial axes, the frequency of the 0-0 separation, and the rotational temperature. The frequencies of the rotational transitions were determined by exact diagonalization of the asymmetric top Hamiltonian.

Pyrazine

In the case of pyrazine, the ground state rotational constants were initially set to literature values[49-52]. Using these same constants as a first approximation for the excited state, and assuming a B-type transition, a spectrum was calculated. This initial spectrum was sufficiently close to the experimental spectrum to allow assignment of many of the transitions. Once these transitions had been assigned, a least squares fitting program and a combination differences program were used to optimize all of the parameters. The best fit calculated spectrum is a B-type spectrum centered at 3069.09 cm^{-1},

and is shown in Figure 2C. The RMS deviation in the fit of the 227 assigned transitions is 15 MHz. More than 200 transitions, however, remained unassigned.

The remaining transitions were assigned by assuming that an additional vibrational band was located in this spectral region. The presence of this second band was evident when the assigned transitions from the first band were subtracted from the experimental spectrum. The remaining transitions formed the second band which is partially overlapped with the first band and is centered at 3067.37 cm^{-1}. The absolute frequencies are measured with a wavemeter with an accuracy of 0.01 cm^{-1}. The relative frequency separation of the two bands, however, is known with the accuracy of our rotational assignments (12 MHz = 4 x 10^{-4} cm^{-1}) to be 1.4130 cm^{-1}. The second band was assigned using the same procedure as the first band and the resulting best fit calculated spectrum is B-type as shown in Figure 2D. Comparison of the two bands reveals that the intensity of the second band is 20% of the first band. The 118 peaks assigned in the second band again fit to the experimental spectrum with an RMS deviation of 15 MHz.

The assignments from the two calculated spectra include all transitions in the experimental spectrum with an intensity greater than 5% of the most intense transition. The spectrum generated by the superposition of the two calculated spectra is shown in Figure 2B. The spectral parameters used to calculate these spectra are given in Table II. The uncertainties reported in Table II were calculated using the procedure described elsewhere, based upon a Monte Carlo simulation of the experimental uncertainties[82]. The assigned transitions in the first (or major) band are given in Table III and the assigned transitions in the second (or minor) band in Table IV.

Naphthalene

The ground state rotational constants for naphthalene were initially set to literature values[69,70]. Using these same constants as a first approximation for the excited state, and assuming a B-type transition a spectrum was calculated. This initial spectrum was not sufficiently close to the experimental spectrum to assign any of the many transitions. The excited state constants were varied using a modified simulated annealing approach[83], until assignments could be made. Once initial assignments had been made the procedure for fitting naphthalene was the same as that for pyrazine. The best fit calculated spectrum is a B-type spectrum centered at 3064.58 cm^{-1}, and is shown in Figure 3B. More than 450 transitions have been assigned and the RMS deviation in the fit is 19 MHz. Figure 4 shows a 0.2 cm^{-1} section of the experimental spectrum and the calculated spectrum. Maior transitions to approximately 40 distinct excited rotational states in the calculated spectrum, however, could not be accounted for in the experimental spectrum.

Local perturbations caused by coupling to another state would account for these "missing" transitions. Mode coupling would result in fragmenting single transitions into two or more transitions. In addition, all transitions to a coupled ro-vibrational state would show the same relative intensity and frequency pattern. Such patterns were found and confirmed by using combination differences. All fragmented transitions indicating mode coupling are given in Table V with the coupling matrix elements. These transitions correspond to three different excited states. The average coupling matrix element was 0.0016 cm^{-1}. A number of additional transitions corresponding to 34 distinct excited states could be assigned as shown in Table VI, but the frequencies of the experimental spectrum deviated from the calculated spectrum by significantly more than the experimental uncertainty.

Combination differences confirmed that the assignments are correct. A further check on assignments was the change in intensity caused by changing the rotational temperature. Spectra with rotational temperatures of approximately 5K and 9K were collected and the intensity changes used to confirm the accuracy of the assignments.

Before concluding that mode coupling was responsible for all deviations from rigid rotor behavior, possible centrifugal distortion effects were investigated. Attempts were made to fit the spectrum using quartic centrifugal distortion constants. The peaks that possess large deviations from the calculated positions continued to deviate even with distortion constants. Thus, we concluded that centrifugal distortion effects were not responsible for the observed perturbations in the spectrum.

The assigned transitions include all transitions in the experimental spectrum with an intensity greater than 15% of the most intense transition. The spectral parameters used to generate the best fit calculated spectrum are given in Table II. The uncertainties reported in Table II were calculated using the procedure described elsewhere, based upon a Monte Carlo simulation of the experimental uncertainties[82]. All assigned transitions for the naphthalene spectrum are given in Table VII.

IV. Discussion

If vibrational mode coupling is the cause of both the second band in the pyrazine spectra and the perturbations in the naphthalene spectra, careful analysis of the two spectra can provide information about the mechanism of mode coupling and the nature of the coupled states. In addition, the

vibrational mode coupling in each molecule will be compared and the similarities or differences will be related to molecular structure and density of states.

Before concluding that the appearance of a second vibrational band in the spectrum of pyrazine is the result of vibrational mode coupling, other alternatives must be eliminated. Other possible explanations are as follows: (1) another vibrational band that coincidentally falls in the same spectral region; (2) a hot band; or (3) a complex. The frequencies of the 24 fundamental modes of pyrazine are given in Table I. The C-H stretching mode discussed here is the ν_{15} mode. There are three other C-H stretching fundamentals, the ν_1 , ν_9 and ν_{19} modes, near the ν_{15} mode. Two of these modes, ν_1 and ν_{19} are not infrared active and the third, ν_9, differs in frequency by 50 cm^{-1}. Furthermore, the symmetries of these other three modes do not produce B-type spectra as observed in the minor band of the experimental spectrum. Combination or overtone bands are expected in this spectral region but are typically much weaker than the fundamental bands. Thus, we conclude that the minor band does not result from the fortuitous overlap of vibrational bands. The other possible causes of the minor band are a hot band or complexes formed in the molecular beam. Hot bands can be eliminated because both bands have the same ground state rotational constants within experimental uncertainty. A vibrational band originating from a thermally populated state is expected to have different rotational constants. Also, hot bands are expected to show a significant dependence on backing pressure, a dependence that was not observed experimentally. Similarly, complexes would be expected to have different ground state rotational constants. As a result, both hot bands and complexes can be eliminated as the cause of the minor band in pyrazine.

After elimination of these other possible explanations, we are left to conclude that the additional band is the result of vibrational mode coupling. In previous work, vibrational mode coupling was also manifested as additional transitions in high resolution spectra. For example, in the spectrum of formamide[1] , vibrational mode coupling manifested itself as two overlapping vibrational bands. By direct analogy between the rotational structure found in the spectra of pyrazine and formamide, the two bands present in the pyrazine spectrum result from the coupling of a single zeroth order dark state and a zeroth order bright state, the C-H stretching mode. Several features in the pyrazine spectrum help to identify the nature of the coupled dark state. The density of states in the vicinity of the C-H stretch, as calculated by a direct counting algorithm is 6 states/cm^{-1} averaged over the frequency interval 3064-3074 cm^{-1}. In this analysis, all of the vibrational modes are treated as uncoupled anharmonic oscillators with 2% anharmonicities. Conservatively, we assume that any state within a 10 cm^{-1} region are candidates for the coupled dark state. Symmetry restrictions reduce the states available for coupling to 7 states. These states are shown in Table VIII.

Having determined that vibrational mode coupling results in doublets in the pyrazine spectrum, the spectrum can be deconvolved using the formalism developed by Lawrence and Knight[84]. This procedure determines the frequencies of the bright state and the perturbing dark state as well as the coupling matrix elements. The utility of this procedure is limited due to its reliance upon both the relative frequencies and relative intensities. We can only reproduce our experimental intensities to 10% of full scale, thus introducing error into the deconvolution procedure. When the peaks are close in frequency, deconvolution does not introduce significant error in the

resulting deconvolved spectra. Our peaks, however, are separated by 1.4130 cm^{-1}, introducing significant error in the deconvolution.

Despite these limitations, some information can be determined about the coupling in the spectrum of pyrazine. We can determine whether the observed spectrum is produced by the coupling of two sets of rigid rotor energy levels, one corresponding to the zeroth order bright state and the other to the zeroth order dark state. This test is performed by noting that the deconvolution is a change of basis set as shown in the matrix transformation in equation 1.

$$\begin{bmatrix} E_L & H' \\ H' & E_D \end{bmatrix} \Leftrightarrow \begin{bmatrix} e_0 & 0 \\ 0 & e_1 \end{bmatrix} \qquad \text{eq 1}$$

where e_0 and e_1 are energies of the molecular eigenstates and E_L and E_D are energies of the zeroth order bright and dark states respectively. H' is the coupling matrix element which couples the bright and dark states. The average energies of the molecular eigenstates will equal the average of the zeroth order energy levels since the trace of a matrix is invariant to transformation. If peaks from two rigid rotor spectra are averaged, the resulting spectrum will be a rigid rotor spectrum[1,85]. Since the spectrum obtained by averaging the frequencies of all the doublets in the spectrum can be fit to a rigid rotor within experimental error (RMS deviation = 15 MHz), the zeroth order states are rigid rotors. If the mechanism of coupling was a rotation-vibration mechanism (such as Coriolis coupling), the coupling of two zeroth order rigid rotors would exhibit a J dependence, resulting in non-rigid rotor behavior in the two observed bands. Since the observed bands are well described by a rigid rotor, we conclude that the mechanism of coupling is anharmonic coupling. The magnitude of the average matrix coupling element has been determined to be 0.36 cm^{-1}.

As in pyrazine, the existence of doublets in the rotational structure in naphthalene are an indication of vibrational mode coupling. For those transitions which were identified as doublets, the average coupling matrix element was determined to be 0.0016 cm^{-1}. Peaks with anomalously large RMS deviations may be the result of longer range interactions where we have been unable to identify all of the molecular eigenstates resulting from the perturbation. Unlike pyrazine, however, it is unlikely that the same zeroth order dark state is responsible for the coupling in all cases. The sporadic appearance of perturbations in the naphthalene spectrum is more suggestive of several different dark states coupling to the bright state. The density of states in the vicinity of the C-H stretch in naphthalene, as calculated by a direct counting algorithm, is 540 states/cm^{-1} averaged over the frequency interval 3060-3070 cm^{-1}. All of the vibrational modes are treated as uncoupled anharmonic oscillators with 2% anharmonicities. Symmetry restrictions reduce the density of states available for coupling to 63 states/cm^{-1}. The large density of states allows for many accidental near degeneracies between the bright state and dark states. Each dark state can have a slightly different geometry, resulting in changes in the rotational constants, which in turn causes the dark states to tune rapidly into and out of resonance. The small coupling constants, in conjunction with the tuning in and out of resonance can cause coupling selectively at individual $J_{K_aK_c}$ states.

As described in the previous section, the observed spectrum of naphthalene is well described by a rigid rotor model, except for several local perturbations in the spectrum. Since many different states are responsible for the coupling, no single coupling mechanism could be identified. The

majority of excited states which exhibit deviations, have large values of K_a, suggestive of Coriolis coupling, but does not rule out other coupling mechanisms.

A comparison of the spectra of pyrazine and naphthalene shows that both molecules are well represented by an asymmetric top/rigid rotor Hamiltonian. Both pyrazine and naphthalene are aromatic ring compounds with a rigid molecular framework. Neither molecule has substituents on its skeletal backbone. Vibrational mode coupling does occur in both molecules, but manifests itself differently. In pyrazine an anharmonic coupling with one other state causes a 1.4130 cm^{-1} splitting of the rotational transitions. Naphthalene, on the other hand, has local perturbations resulting from fortuitous near degeneracies with a variety of states. These perturbations are seen as the splitting of some states and deviations in energy from the rigid rotor model for other states.

The differences in the mode coupling in pyrazine and naphthalene cannot be explained using density of states arguments. The relative density of symmetry allowed states for pyrazine and naphthalene are 1 and 63 states/cm^{-1} respectively. Thus, density of states arguments would predict that there would be significantly more coupling in naphthalene than in pyrazine—a difference that is not observed experimentally. Pyrazine, the lower density of states molecule, has stronger coupling to a single state (matrix element = 0.36 cm^{-1}), while naphthalene exhibits only very weak sporadic coupling (matrix element = 0.001 cm^{-1}). Even if one discounts the relatively large coupling, to a single state, observed in pyrazine as resulting from a fortuitous near resonance of a strongly coupled state, the differences observed are not consistent with the differences in the density of states.

Further insight concerning mode coupling and density of states is provided by a comparison of naphthalene and 2-fluoroethanol (2FE). Both of these molecules have a similar density of symmetry allowed states, approximately 60 states/cm^{-1}. In addition, the spectra of both molecules exhibit peak fractionation signaling mode coupling. The average coupling matrix element of naphthalene and 2FE are 0.001 and 0.003 cm^{-1}, respectively. Using density of states arguments, these two molecules are predicted to exhibit very similar coupling behavior. Such similarities are not observed. While naphthalene exhibits occasional coupling to other states sporadically throughout the spectrum, 2FE couples to every available state, throughout the spectrum. This dramatic difference in coupling behavior is not consistent with density of states arguments.

The most obvious structural difference between naphthalene and 2FE is the presence of the torsional mode in 2FE. Torsional quanta are present in over 90% of the dark states involved in coupling in 2FE. There are no analogous low frequency, large amplitude modes in naphthalene comparable to torsions. The motion described by ring deformation modes, that have similar frequencies to torsions, do not involve intramolecular interactions. In contrast, the motion described by torsions involve intramolecular interactions between the CH_2F group and the CH_2OH group. These kinds of intramolecular interactions have been suggested to enhance vibrational mode coupling, both by the work of Parmenter and coworkers[20,21,86,87] and by previous work in our group[5-9,23]. Thus, we conclude that molecular structure rather than density of states models are required to explain the relative coupling in pyrazine, naphthalene and substituted ethanes.

In conclusion, a detailed analysis of the rotational spectrum of the C-H stretching mode in both pyrazine and naphthalene has demonstrated the

presence of vibrational mode coupling. The vibrational mode coupling in the two molecules have a number of important differences. The coupling in pyrazine occurs via an anharmonic mechanism to a single dark state which manifests itself as a splitting of every rotational transition into doublets 1.4130 cm^{-1} apart. The coupling in naphthalene occurs to a variety of dark states and is manifested as weak, local perturbations. The coupling in pyrazine is also two orders of magnitude stronger than the coupling in naphthalene. The observed differences in mode coupling are not consistent with density of states arguments. Structural arguments, particularly the lack of low frequency, large amplitude torsional motions, more effectively describes the relative mode coupling observed in these two planar ring systems as compared to substituted ethanes.

Acknowledgments: The authors would like to thank C. Cameron Miller and Hao Li for several helpful discussions and suggestions. They would also like to thank Julian Hjortshøj for help in using the modified simulated annealing software and Steve Stone for his help in the naphthalene data acquisition. This work is supported by: The National Institute of Health under grant #08-R9N527039A, The Office of Naval Research under grant #N00014-90-J-1971, and The Petroleum Research Fund administered by the American Chemical Society.

References

(1) C. L. Brummel, M. Shen, K. B. Hewett and L. A. Philips, J. Opt. Soc. Am. B, (in press).

(2) R. E. Miller, Acc. Chem. Res., **23**, 10-16 (1990).

(3) K. W. Jucks and R. E. Miller, J. Chem. Phys., **86**, 6637-6645 (1987).

(4) J. Go, G. A. Bethardy and D. S. Perry, J. Phys. Chem., **94**, 6153-6156 (1990).

(5) C. L. Brummel, S. W. Mork and L. A. Philips, J. Chem. Phys., **95**, 7041-7053 (1991).

(6) C. L. Brummel, S. W. Mork and L. A. Philips, J. Am. Chem. Soc., **113**, 4342-4343 (1991).

(7) S. W. Mork, C. C. Miller and L. A. Philips, J. Chem. Phys., **97**, 2971-2981 (1992).

(8) C. C. Miller, M. Shen and L. A. Philips, J. Phys. Chem., **97**, 537-539 (1993).

(9) C. C. Miller, S. C. Stone and L. A. Philips, J. Chem. Phys., (in preparation).

(10) H. Li, C. C. Miller and L. A. Philips, J. Chem. Phys., (submitted).

(11) A. M. de Souza, D. Kaur and D. S. Perry, J. Chem. Phys., **88**, 4569-4578 (1988).

(12) G. A. Bethardy and D. S. Perry, J. Mol. Spectrosc., **144**, 304-309 (1990).

(13) A. McIlroy and D. J. Nesbitt, J. Chem. Phys., **91**, 104-113 (1989).

(14) A. McIlroy and D. J. Nesbitt, J. Chem. Phys., **92**, 2229-2243 (1990).

(15) K. K. Lehmann, B. H. Pate and G. Scoles, J. Chem. Phys., **93**, 2152-2153 (1990).

(16) B. H. Pate, K. K. Lehmann and G. Scoles, J. Chem. Phys., **95**, 3891-3916 (1991).

(17) E. R. Th. Kerstel, K. K. Lehmann, T. F. Mentel, B. H. Pate and G. Scoles, J. Phys. Chem., **95**, 8282-8293 (1991).

(18) R. D. Levine and J. Jortner, "Mode Selective Chemistry"; in *Mode Selective Chemistry*, edited by J. Jortner, R. D. Levine and B. Pullman (Kluwer Academic Publishers, Boston, 1991) pp. 535-571.

(19) C. C. Miller, L. A. Philips, A. M. Andrews, G. T. Fraser, B. H. Pate and R. D. Suenram, J. Chem. Phys., (in press).

(20) C. S. Parmenter and B. M. Stone, J. Chem. Phys., **84**, 4710-4711 (1986).

(21) D. B. Moss and C. S. Parmenter, J. Chem. Phys., **98**, 6897-6905 (1993).

(22) G. A. Bethardy, X. Wang and D. S. Perry, (unpublished manuscript).

(23) H. Li, G. S. Ezra and L. A. Philips, J. Chem. Phys., **97**, 5956-5963 (1992).

(24) S. Califano, G. Adembri and G. Sbrana, Spectrochim. Acta, **20**, 385-396 (1964).

(25) R. C. Lord, A. L. Marston and F. A. Miller, Spectrochim. Acta, **9**, 113-125 (1957).

(26) J. D. Simmons, K. K. Innes and G. M. Begun, J. Mol. Spectrosc., **14**, 190-197 (1964).

(27) G. Sbrana, V. Schettino and R. Righini, J. Chem. Phys., **59**, 2441-2450 (1973).

(28) J. Zarembowitch and L. Bokobza-Sebagh, Spectrochim. Acta, **32A**, 605-615 (1976).

(29) M. Ito, I. Suzuka, Y. Udagawa, N. Mikami and K. Kaya, Chem. Phys. Lett., **16**, 211-213 (1972).

(30) H.-K. Hong and C. W. Jacobsen, J. Chem. Phys., **68**, 1170-1184 (1978).

(31) V. Schomaker and L. Pauling, J. Am. Chem. Soc., **61**, 1769-1780 (1939).

(32) S. Cradock, P. B. Liescheski, D. W. H. Rankin and H. E. Robertson, J. Am. Chem. Soc., **110**, 2758-2763 (1988).

(33) P. J. Wheatley, Acta Crystallogr., **10**, 182-187 (1957).

(34) G. C. Pimentel and A. L. McClellan, J. Chem. Phys., **20**, 270-277 (1952).

(35) V. H. Luther, G. Brandes, H. Günzler and B. Hampel, Z. Elektrochem., **59**, 1012-1022 (1955).

(36) W. B. Person, G. C. Pimentel and O. Schnepp, J. Chem. Phys., **23**, 230-233 (1955).

(37) G. C. Pimentel, A. L. McClellan, W. B. Person and O. Schnepp, J. Chem. Phys., **23**, 234-237 (1955).

(38) H. Sellers, P. Pulay and J. E. Boggs, J. Am. Chem. Soc., **107**, 6487-6494 (1985).

(39) E. R. Lippincott and E. J. O'Reilly Jr., J. Chem. Phys., **23**, 238-244 (1955).

(40) A. L. McClellan and G. C. Pimentel, J. Chem. Phys., **23**, 245-248 (1955).

(41) S. S. Mitra and H. J. Bernstein, Can. J. Chem., **37**, 553-562 (1959).

(42) I. Harada and T. Shimanouchi, J. Chem. Phys., **44**, 2016-2028 (1966).

(43) H. Yamada and K. Suzuki, Spectrochim. Acta, **23A**, 1735-1744 (1967).

(44) K. Tsuji and H. Yamada, J. Phys. Chem., **76**, 260-269 (1972).

(45) M. Hineno and H. Yoshinaga, Spectrochim. Acta, **31A**, 617-620 (1975).

(46) J. A. Duckett, T. L. Smithson and H. Wieser, J. Mol. Struct., **44**, 97-99 (1978).

(47) S. C. Abrahams, J. M. Robertson and J. G. White, Acta Crystallogr., **2**, 233-238 (1949).

(48) S. C. Abrahams, J. M. Robertson and J. G. White, Acta Crystallogr., **2**, 238-244 (1949).

(49) K. K. Innes, J. P. Byrne and I. G. Ross, J. Mol. Spectrosc., **22**, 125-147 (1967).

(50) J. A. Merritt and K. K. Innes, Spectrochim. Acta, **16**, 945-953 (1960).

(51) K. K. Innes and J. E. Parkin, J. Mol. Spectrosc., **21**, 66-75 (1966).

(52) K. K. Innes, A. H. Kalantar, A. Y. Khan and T. J. Durnick, J. Mol. Spectrosc., **43**, 477-482 (1972).

(53) D. B. McDonald and S. A. Rice, J. Chem. Phys., **74**, 4893-4906 (1981).

(54) P.-N. Wang, E. C. Lim and W. Siebrand, Chem. Phys. Lett., **159**, 7-9 (1989).

(55) S. Hillenbrand, L. Zhu and P. Johnson, J. Chem. Phys., **95**, 2237-2243 (1991).

(56) P. U. de Haag, J. Heinze and W. L. Meerts, Chem. Phys. Lett., **177**, 357-360 (1991).

(57) J. Kommandeur, W. A. Majewski, W. L. Meerts and D. W. Pratt, Ann. Rev. Phys. Chem., **38**, 433-462 (1987).

(58) J. Kommandeur, Advan. Chem. Phys., **70**, 133-164 (1988).

(59) P. J. de Lange, B. J. van der Meer, K. E. Drabe, J. Kommandeur, W. L. Meerts and W. A. Majewski, J. Chem. Phys., **86**, 4004-4010 (1987).

(60) N. Mikami, H. Igarashi, K. Kaya and M. Ito, Bull. Chem. Soc., Jpn., **55**, 374-379 (1982).

(61) D. B. McDonald, G. R. Fleming and S. A. Rice, Chem. Phys., **60**, 335-345 (1981).

(62) A. Amirav, Chem. Phys., **108**, 403-416 (1986).

(63) A. Amirav, Chem. Phys., **126**, 365-375 (1988).

(64) A. Amirav, Chem. Phys., **126**, 327-342 (1988).

(65) A. Amirav and Y. Oreg, Chem. Phys., **126**, 343-364 (1988).

(66) H. Baba, M. Fujita and K. Uchida, Chem. Phys. Lett., **73**, 425-428 (1980).

(67) H. Baba, N. Ohta, O. Sekiguchi, M. Fujita and K. Uchida, J. Phys. Chem., **87**, 943-952 (1983).

(68) Y. Matsumoto, L. H. Spangler and D. W. Pratt, Chem. Phys. Lett., **98**, 333-339 (1983).

(69) W. Majewski and W. L. Meerts, J. Mol. Spectrosc., **104**, 271-281 (1984).

(70) J. M. Hollas and S. N. Thakur, Mol. Phys., **22**, 203-212 (1971).

(71) A. E. W. Knight, B. J. Selinger and I. G. Ross, Aust. J. Chem., **26**, 1159-1172 (1973).

(72) J. C. Hsieh, C.-S. Huang and E. C. Lim, J. Chem. Phys., **60**, 4345-4353 (1974).

(73) W. E. Howard and E. W. Schlag, Chem. Phys., **17**, 123-138 (1976).

(74) L. M. Hall, T. F. Hunter and M. G. Stock, Chem. Phys. Lett., **44**, 145-149 (1976).

(75) S. M. Beck, D. L. Monts, M. G. Liverman and R. E. Smalley, J. Chem. Phys., **70**, 1062-1063 (1979).

(76) S. M. Beck, D. E. Powers, J. B. Hopkins and R. E. Smalley, J. Chem. Phys., **73**, 2019-2028 (1980).

(77) S. M. Beck, J. B. Hopkins, D. E. Powers and R. E. Smalley, J. Chem. Phys., **74**, 43-52 (1981).

(78) C. A. Langhoff and G. W. Robinson, Chem. Phys., **6**, 34-53 (1974).

(79) F. M. Behlen, D. B. McDonald, V. Sethuraman and S. A. Rice, J. Chem. Phys., **75**, 5685-5693 (1981).

(80) D. P. Craig, J. M. Hollas, M. F. Redies and S. C. Wait Jr., Phil. Trans. Roy. Soc. London, **A253**, 543-568 (1961).

(81) K. K. Innes, J. E. Parkin, D. K. Ervin, J. M. Hollas and I. G. Ross, J. Mol. Spectrosc., **16**, 406-414 (1965).

(82) C. L. Brummel and L. A. Philips, J. Mol. Spectrosc., **159**, 287-299 (1993).

(83) J. M. Hjortshøj and L. A. Philips, J. Mol. Spectrosc., **154**, 288-304 (1992).

(84) W. D. Lawrence and A. E. W. Knight, J. Phys. Chem., **89**, 917-925 (1985).

(85) If two rigid rotor spectra are averaged peak for peak the resulting new spectrum will be well characterized by a rigid rotor. If the difference in the rotational constants of the two original spectra is small the rotational constants for the average spectrum will be the average of the rotational constants of the original spectra.

(86) C. S. Parmenter, J. Phys. Chem., **86**, 1735-1750 (1982).

(87) C. S. Parmenter, Faraday Discuss. Chem. Soc., **75**, 7-22 (1983).

Figure Captions

Figure 1: The figure shows the molecular structure of pyrazine and naphthalene and the axis system used to assign symmetry labels under the D_{2h} point group. In both molecules the inertial axes are correlated with the given axis system (A to Z and B to Y).

Figure 2: The figure shows the experimental spectrum of pyrazine (A) and the best fit to the experimental spectrum (B). The best fit calculated spectrum consists of the superposition of 2 bands, a major band shown in panel C and a minor band shown in panel D.

Figure 3: The figure shows the experimental spectrum of naphthalene (A) and the best fit to the experimental spectrum (B). The calculated spectrum has a rotational temperature of 9 K.

Figure 4: The figure shows a 0.2 cm^{-1} section of the naphthalene spectrum and the calculated spectrum. The peaks marked with a (♦) have been assigned.

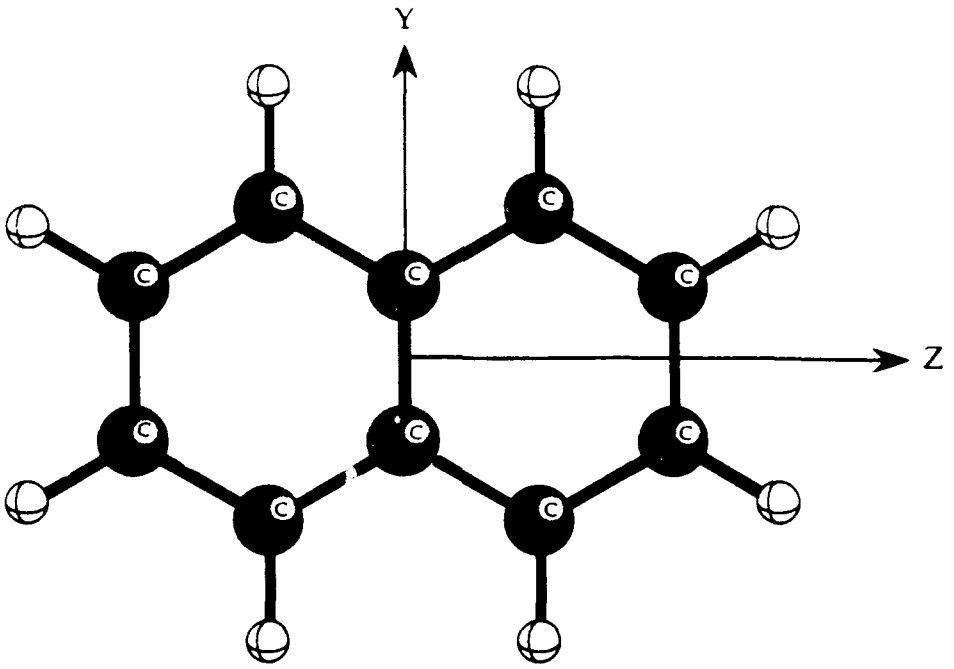

Naphthalene

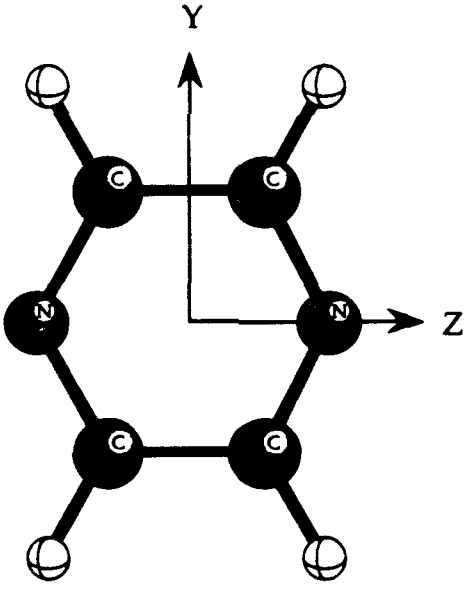

Pyrazine

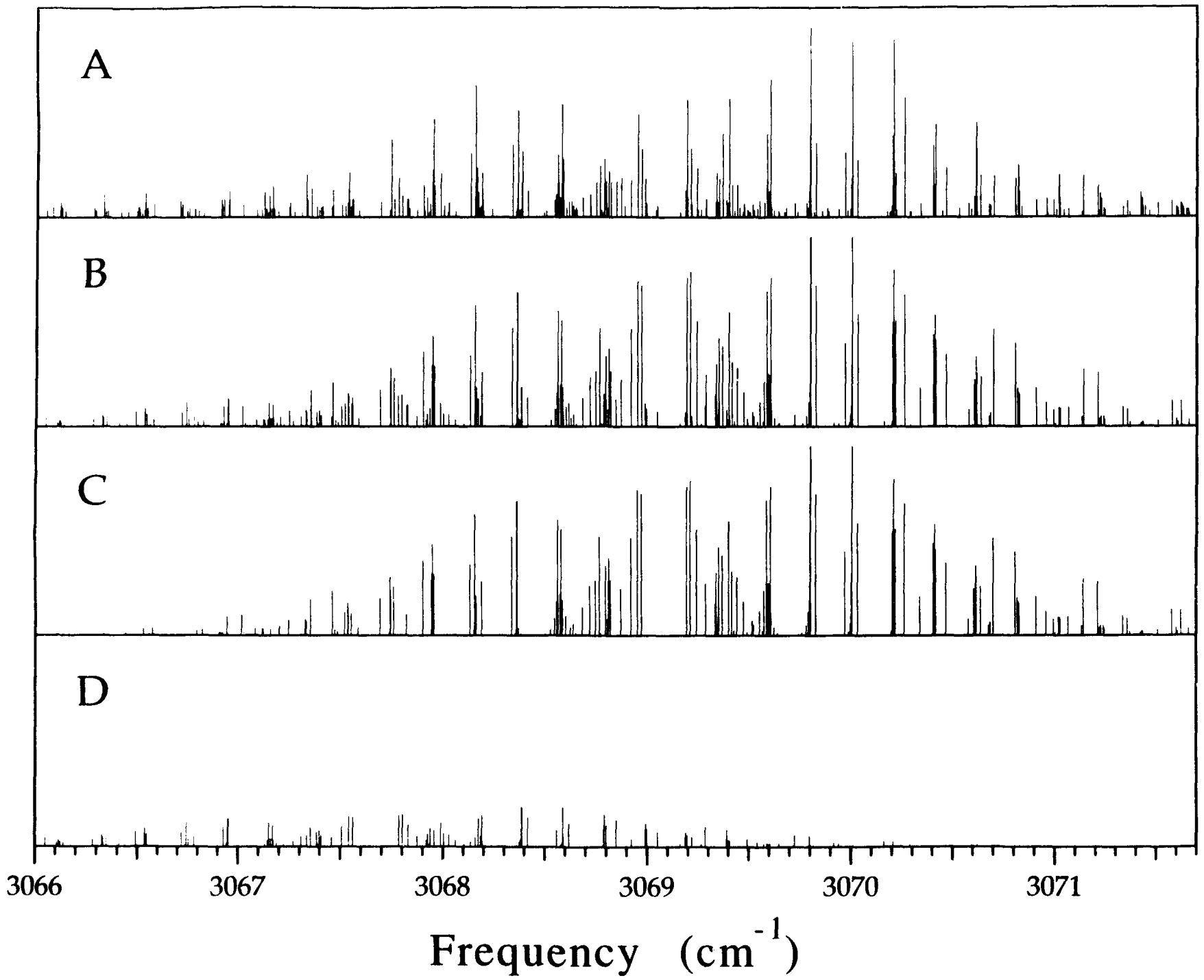
A
B
C
D
3066
3067
3068
3069
3070
3071
Frequency (cm-1)

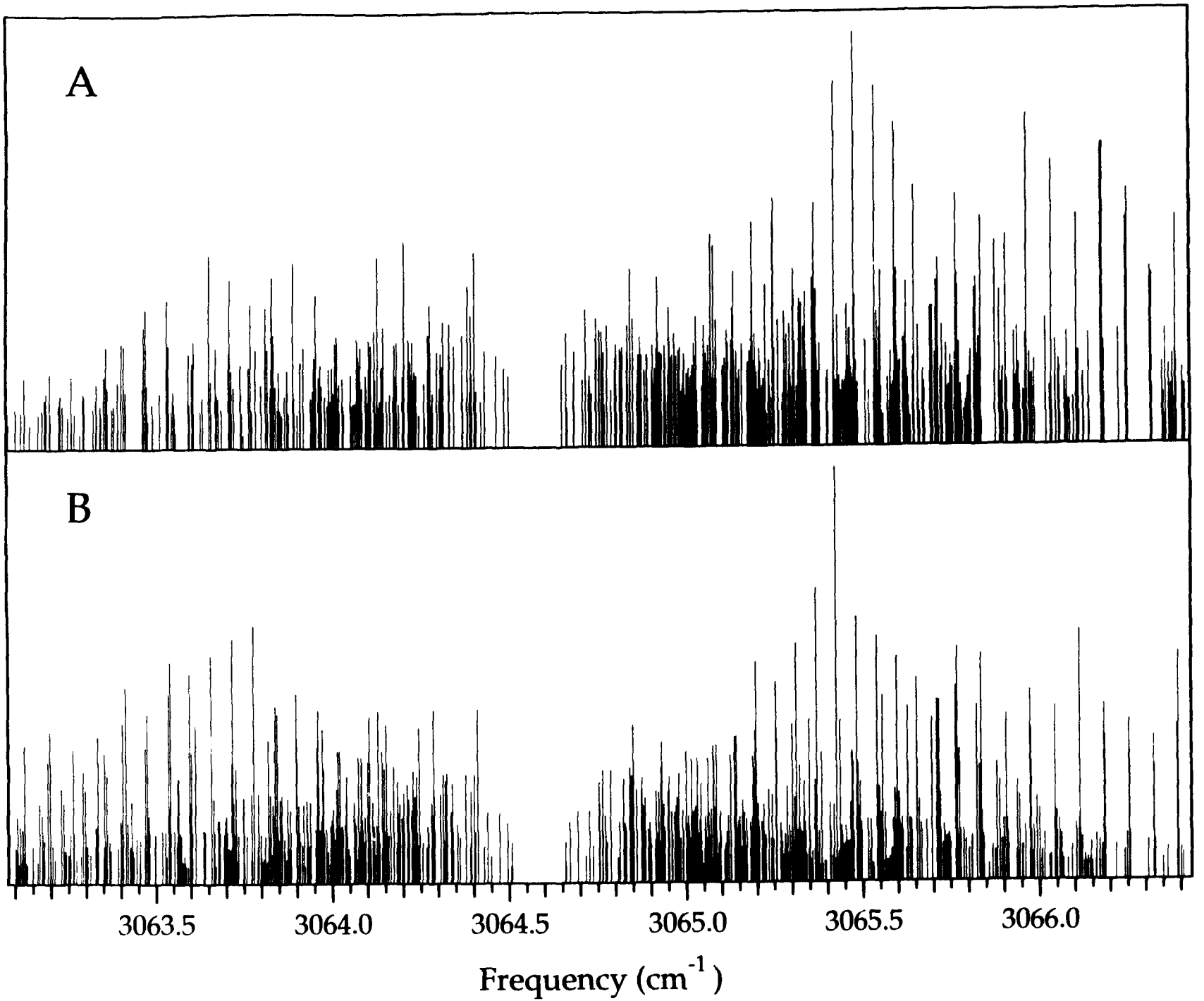
A
B
3063.5
3064.0
3064.5
3065.0
3065.5
3066.0
Frequency (cm-1)

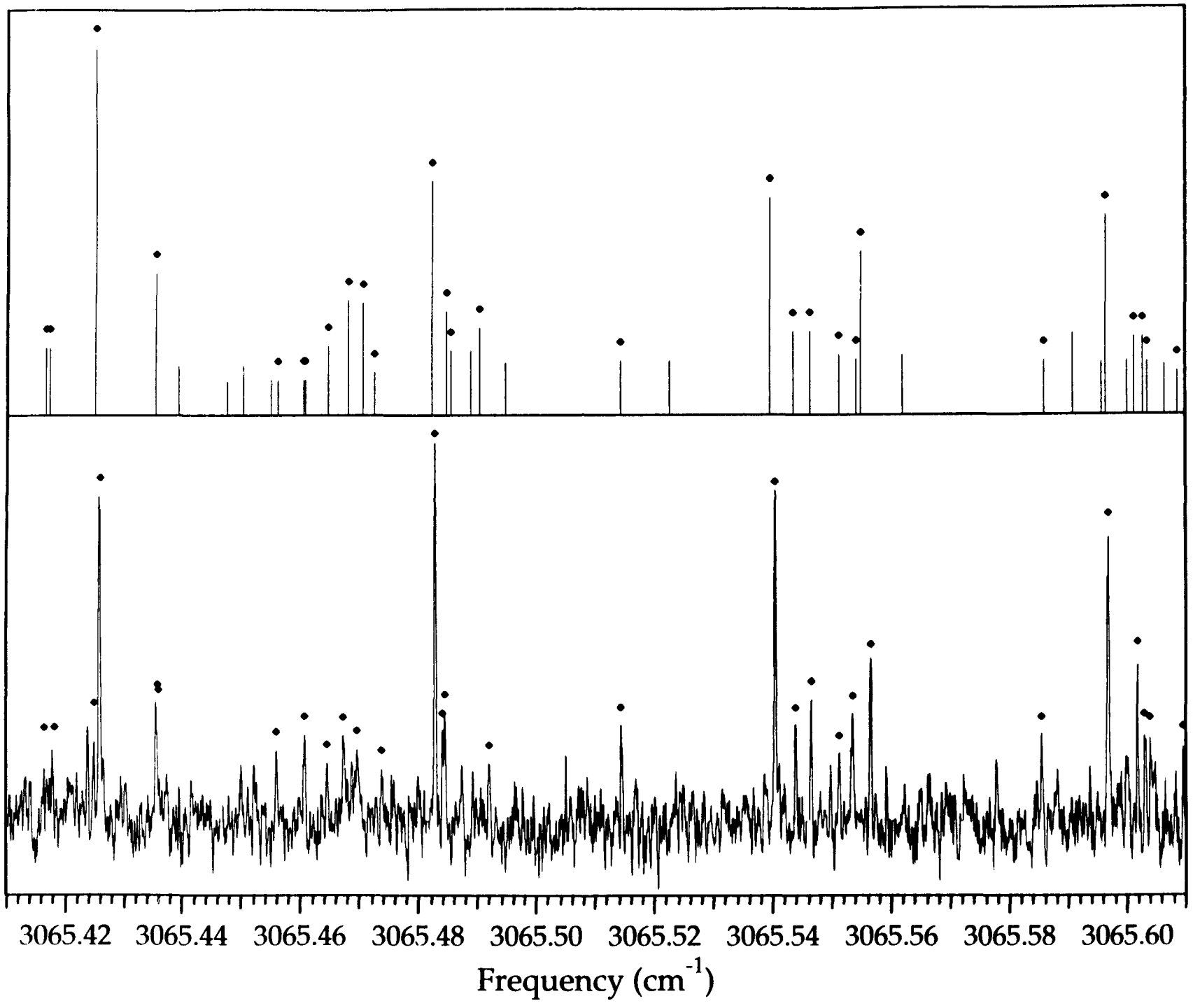
3065.42
3065.44
3065.46
3065.48
3065.50
3065.52
3065.54
3065.56
3065.58
3065.60
Frequency (cm-1)

Table I: This table compares the fundamental vibrations of pyrazine and naphthalene. The pyrazine fundamentals are from reference 28 and the naphthalene fundamentals are from reference 38 unless noted otherwise.

	Pyrazine		Naphthalene		
	Vibration	Frequency (cm^{-1})	Vibration	Frequency (cm^{-1})	
A_g	1	3055	1	3060[a]	C-H stretch
			2	3030[a]	
	2	1580	3	1578	C-C stretch
			4	1460	
	3	1233	5	1380	C-H bend
			6	1163	
	4	1016	7	1020	ring breathing
	5	602	8	757	ring deformation
			9	505	
A_u	6	960	10	981[b]	oop[c] C-H bend
			11	825[b]	
	7	350	12	622[b]	oop ring deformation
			13	188[b]	
B_{1g}	8	927	14	951	oop C-H bend
			15	717	
			16	385	oop skeletal bend
B_{1u}	9	3012	17	3060[a]	C-H stretch
			18	3027[a]	
	10	1483	19	1595	C-C stretch
			20	1389	
	11	1130	21	1265	C-H bend
			22	1125	
	12	1018	23	789[d]	ring deformation
			24	359	
B_{2g}	13	983	25	983	oop C-H bend
			26	875	
	14	756	27	772	oop skeletal bend
			28	470	
B_{2u}	15	3069.09[e]	29	3064.58[f]	C-H stretch
			30	2987[a]	
	16	1411	31	1509	C-C stretch
			32	1361	
	17	1149	35	1008	ring deformation
			36	619	
	18	1063	33	1209	C-H bend
			34	1163	

B_{3g}	19	3040	37	3092[a]	C-H stretch
			38	2978[a]	
	20	1525	39	1624	C-C stretch
			40	1458	
	21	1346	41	1240	C-H bend
			42	1158	
	22	704	43	939	skeletal deformation
			44	508	
B_{3u}	23	785	45	955	oop C-H bend
			46	780	
	24	418	47	474	oop skeletal bend
			48	176	oop wing-wagging

[a]From reference 41.

[b]Calculated values.

[c]oop indicates out-of-plane vibration.

[d]Value obtained from extrapolation of perdeuterated naphthalene and calculations.

[e]Center of major pyrazine band from this work.

[f]Center of naphthalene band from this work.

Table II: The best fit rotational constants for pyrazine and naphthalene as determined in this work. The uncertainties are for the 94.5% confidence limit. All values are in cm^{-1}.

	Pyrazine		
	Ground State	Excited State Major Transition	Excited State Minor Transition
A	0.213824 (13)	0.2135972 (95)	0.213612 (45)
B	0.197304 (13)	0.1970904 (81)	0.196863 (40)
C	0.1026078 (83)	0.1024339 (18)	0.1022168 (75)
Center Frequency		3069.09 (2)	3067.67 (2)

	Naphthalene	
	Ground State	Excited State
A	0.103949 (17)	0.104013 (17)
B	0.0411050 (55)	0.0411023 (45)
C	0.0294689 (41)	0.0294062 (20)
Center Frequency		3064.58 (2)

Table III: Pyrazine transitions assigned to the major band. The intensity is relative to the largest transition in the spectrum. The RMS deviation of the fit is 15 MHz.

Frequency (cm^{-1})	Intensity	$J'_{Ka'\ Kc'}$	$J''_{Ka''\ Kc''}$
3072.03702	7.56	$7_{7\,0}$	$6_{6\,1}$
3072.01027	10.46	$7_{7\,1}$	$6_{6\,0}$
3071.84852	2.94	$5_{3\,3}$	$4_{0\,4}$
3071.84398	4.67	$5_{2\,3}$	$4_{1\,4}$
3071.84296	2.41	$9_{5\,5}$	$8_{4\,4}$
3071.83886	2.30	$9_{4\,5}$	$8_{5\,4}$
3071.83543	6.40	$10_{4\,7}$	$9_{3\,6}$
		$10_{3\,7}$	$9_{4\,6}$
3071.83191	6.24	$11_{3\,9}$	$10_{2\,8}$
		$11_{2\,9}$	$10_{3\,8}$
3071.82895	5.33	$12_{2\,11}$	$11_{1\,10}$
		$12_{1\,11}$	$11_{2\,10}$
3071.82575	6.50	$13_{1\,13}$	$12_{0\,12}$
		$13_{0\,13}$	$12_{1\,12}$
3071.81039	2.63	$7_{6\,2}$	$6_{5\,1}$
3071.70965	7.25	$6_{5\,1}$	$5_{4\,2}$
3071.66199	2.57	$5_{4\,2}$	$4_{1\,3}$
3071.65873	4.52	$8_{5\,4}$	$7_{4\,3}$
3071.63509	4.00	$9_{4\,6}$	$8_{3\,5}$
		$9_{3\,6}$	$8_{4\,5}$
3071.63248	5.13	$10_{3\,8}$	$9_{2\,7}$
		$10_{2\,8}$	$9_{3\,7}$
3071.62761	6.16	$11_{2\,10}$	$10_{1\,9}$
		$11_{1\,10}$	$10_{2\,9}$
3071.62633	3.31	$8_{4\,4}$	$7_{5\,3}$
3071.62500	7.01	$12_{1\,12}$	$11_{0\,11}$
		$12_{0\,12}$	$11_{1\,11}$
3071.62238	7.91	$6_{6\,0}$	$5_{5\,1}$
3071.60033	5.77	$5_{3\,2}$	$4_{2\,3}$
3071.57725	8.83	$6_{6\,1}$	$5_{5\,0}$
3071.50822	7.66	$7_{5\,3}$	$6_{4\,2}$
3071.43410	5.04	$8_{4\,5}$	$7_{3\,4}$
3071.43265	6.18	$8_{3\,5}$	$7_{4\,4}$
3071.42953	9.87	$9_{3\,7}$	$8_{2\,6}$
		$9_{2\,7}$	$8_{3\,6}$
3071.42659	9.99	$10_{2\,9}$	$9_{1\,8}$
		$10_{1\,9}$	$9_{2\,8}$
3071.42396	12.83	$11_{1\,11}$	$10_{0\,10}$
		$11_{0\,11}$	$10_{1\,10}$
3071.36865	2.96	$7_{4\,3}$	$6_{5\,2}$
3071.35777	8.53	$6_{5\,2}$	$5_{4\,1}$
3071.33516	5.58	$5_{4\,1}$	$4_{3\,2}$
3071.24449	4.15	$4_{3\,2}$	$3_{0\,3}$
3071.23918	4.68	$7_{4\,4}$	$6_{3\,3}$
3071.22874	9.50	$8_{3\,6}$	$7_{2\,5}$
		$8_{2\,6}$	$7_{3\,5}$
3071.22663	9.56	$7_{3\,4}$	$6_{4\,3}$
3071.22607	5.43	$9_{2\,8}$	$8_{1\,7}$
		$9_{1\,8}$	$8_{2\,7}$
3071.22232	12.68	$10_{1\,10}$	$9_{0\,9}$
		$10_{0\,10}$	$9_{1\,9}$
3071.21650	3.37	$4_{2\,2}$	$3_{1\,3}$
3071.21209	16.75	$5_{5\,0}$	$4_{4\,1}$
3071.13998	21.78	$5_{5\,1}$	$4_{4\,0}$
3071.13246	2.82	$4_{4\,1}$	$3_{1\,2}$
3071.06732	4.73	$6_{4\,3}$	$5_{3\,2}$
3071.02520	9.88	$7_{3\,5}$	$6_{2\,4}$
3071.02485	4.12	$7_{2\,5}$	$6_{3\,4}$
3071.02215	16.21	$8_{2\,7}$	$7_{1\,6}$
		$8_{1\,7}$	$7_{2\,6}$
3071.01988	22.55	$9_{1\,9}$	$8_{0\,8}$
		$9_{0\,9}$	$8_{1\,8}$
3070.99452	9.08	$6_{3\,3}$	$5_{4\,2}$
3070.95903	9.90	$4_{3\,1}$	$3_{2\,2}$
3070.90914	9.18	$5_{4\,2}$	$4_{3\,1}$
3070.82609	13.46	$6_{3\,4}$	$5_{2\,3}$
3070.82184	21.11	$7_{2\,6}$	$6_{1\,5}$
		$7_{1\,6}$	$6_{2\,5}$
3070.82152	9.01	$6_{2\,4}$	$5_{3\,3}$
3070.81985	27.64	$8_{0\,8}$	$7_{1\,7}$
		$8_{1\,8}$	$7_{0\,7}$
3070.80710	20.47	$4_{4\,0}$	$3_{3\,1}$
3070.70141	21.84	$4_{4\,1}$	$3_{3\,0}$
3070.68477	6.28	$5_{3\,2}$	$4_{4\,1}$

3070.67926	6.98	$3_{3\,1}$	$2_{0\,2}$
3070.63746	22.30	$5_{3\,3}$	$4_{2\,2}$
3070.61783	36.25	$6_{2\,5}$	$5_{1\,4}$
		$6_{1\,5}$	$5_{2\,4}$
3070.61569	49.75	$7_{1\,7}$	$6_{0\,6}$
		$7_{0\,7}$	$6_{1\,6}$
3070.61201	4.62	$8_{1\,7}$	$8_{0\,8}$
		$8_{2\,7}$	$8_{1\,8}$
3070.60699	3.80	$9_{2\,7}$	$9_{1\,8}$
		$9_{3\,7}$	$9_{2\,8}$
3070.60573	10.99	$5_{2\,3}$	$4_{3\,2}$
3070.57843	7.37	$3_{2\,1}$	$2_{1\,2}$
3070.46776	26.04	$4_{3\,2}$	$3_{2\,1}$
3070.41547	18.49	$5_{2\,4}$	$4_{1\,3}$
3070.41459	48.77	$6_{1\,6}$	$5_{0\,5}$
		$6_{0\,6}$	$5_{1\,5}$
3070.41426	31.48	$5_{1\,4}$	$4_{2\,3}$
3070.40773	16.98	$7_{2\,6}$	$7_{1\,7}$
		$7_{1\,6}$	$7_{0\,7}$
3070.40448	37.90	$3_{3\,0}$	$2_{2\,1}$
3070.34085	7.34	$4_{2\,2}$	$3_{3\,1}$
3070.26303	62.69	$3_{3\,1}$	$2_{2\,0}$
3070.21740	23.13	$4_{2\,3}$	$3_{1\,2}$
3070.20946	93.08	$5_{1\,5}$	$4_{0\,4}$
		$5_{0\,5}$	$4_{1\,4}$
3070.20608	43.01	$4_{1\,3}$	$3_{2\,2}$
3070.20162	5.99	$7_{2\,5}$	$7_{1\,6}$
		$7_{3\,5}$	$7_{2\,6}$
3070.19614	3.34	$8_{3\,5}$	$8_{2\,6}$
		$8_{4\,5}$	$8_{3\,6}$
3070.18943	3.10	$9_{4\,5}$	$9_{3\,6}$
3070.17878	3.21	$10_{5\,5}$	$10_{4\,6}$
3070.03334	30.18	$3_{2\,2}$	$2_{1\,1}$
3070.00577	92.23	$4_{1\,4}$	$3_{0\,3}$
		$4_{0\,4}$	$3_{1\,3}$
3070.00341	20.65	$2_{2\,0}$	$1_{1\,1}$
3070.00277	12.75	$5_{1\,4}$	$5_{0\,5}$
		$5_{2\,4}$	$5_{1\,5}$
3069.99861	4.53	$6_{3\,4}$	$6_{2\,5}$
3069.98299	3.87	$8_{4\,4}$	$8_{3\,5}$

3069.97370	34.06	$3_{1\,2}$	$2_{2\,1}$
3069.82926	39.16	$2_{2\,1}$	$1_{1\,0}$
3069.80306	100.00	$3_{1\,3}$	$2_{0\,2}$
3069.80099	48.45	$3_{0\,3}$	$2_{1\,2}$
3069.79967	12.18	$4_{2\,3}$	$4_{1\,4}$
3069.79876	14.34	$4_{1\,3}$	$4_{0\,4}$
3069.79669	9.48	$5_{3\,3}$	$5_{2\,4}$
3069.79346	2.66	$6_{4\,3}$	$6_{3\,4}$
3069.79288	5.15	$5_{2\,3}$	$5_{1\,4}$
3069.78200	7.75	$6_{3\,3}$	$6_{2\,4}$
3069.64470	3.77	$7_{6\,2}$	$7_{5\,3}$
3069.62447	3.82	$6_{5\,2}$	$6_{4\,3}$
3069.61056	5.61	$5_{4\,2}$	$5_{3\,3}$
3069.60648	72.30	$2_{1\,2}$	$1_{0\,1}$
3069.60288	13.68	$4_{3\,2}$	$4_{2\,3}$
3069.59969	13.82	$3_{2\,2}$	$3_{1\,3}$
3069.59062	19.09	$3_{1\,2}$	$3_{0\,3}$
3069.58854	43.99	$2_{0\,2}$	$1_{1\,1}$
3069.57661	8.16	$4_{2\,2}$	$4_{1\,3}$
3069.55371	8.86	$5_{3\,2}$	$5_{2\,3}$
3069.52532	4.05	$6_{4\,2}$	$6_{3\,3}$
3069.51858	6.85	$5_{5\,1}$	$5_{4\,2}$
3069.47696	7.37	$4_{4\,1}$	$4_{3\,2}$
3069.46915	2.93	$8_{6\,2}$	$8_{5\,3}$
3069.45383	5.46	$9_{7\,2}$	$9_{6\,3}$
3069.44370	17.40	$3_{3\,1}$	$3_{2\,2}$
3069.42838	3.59	$6_{6\,0}$	$6_{5\,1}$
3069.41874	17.22	$2_{2\,1}$	$2_{1\,2}$
3069.40261	62.60	$1_{1\,1}$	$0_{0\,0}$
3069.37158	44.27	$2_{1\,1}$	$2_{0\,2}$
3069.35466	20.54	$3_{2\,1}$	$3_{1\,2}$
3069.35198	7.34	$5_{5\,0}$	$5_{4\,1}$
3069.34555	8.28	$6_{5\,1}$	$6_{4\,2}$
3069.34081	23.61	$4_{3\,1}$	$4_{2\,2}$
3069.33647	8.20	$5_{4\,1}$	$5_{3\,2}$
3069.28970	9.83	$4_{4\,0}$	$4_{3\,1}$
3069.24487	26.02	$3_{3\,0}$	$3_{2\,1}$

3069.21504	36.33	$2_{2\,0}$	$2_{1\,1}$
3069.19761	62.03	$1_{1\,0}$	$1_{0\,1}$
3068.97524	35.93	$1_{0\,1}$	$1_{1\,0}$
3068.95600	54.02	$2_{1\,1}$	$2_{2\,0}$
3068.92277	19.45	$3_{2\,1}$	$3_{3\,0}$
3068.87456	20.60	$4_{3\,1}$	$4_{4\,0}$
3068.82344	18.53	$5_{3\,2}$	$5_{4\,1}$
		$4_{2\,2}$	$4_{3\,1}$
3068.81359	24.51	$3_{1\,2}$	$3_{2\,1}$
3068.80938	4.35	$6_{4\,2}$	$6_{5\,1}$
3068.80800	4.62	$5_{4\,1}$	$5_{5\,0}$
3068.79923	18.79	$2_{0\,2}$	$2_{1\,1}$
3068.77724	3.80	$7_{5\,2}$	$7_{6\,1}$
3068.77009	27.10	$0_{0\,0}$	$1_{1\,1}$
3068.75197	18.38	$2_{1\,2}$	$2_{2\,1}$
3068.72472	12.26	$3_{2\,2}$	$3_{3\,1}$
3068.68762	10.69	$4_{3\,2}$	$4_{4\,1}$
3068.64127	6.32	$5_{4\,2}$	$5_{5\,1}$
3068.63081	8.55	$6_{3\,3}$	$6_{4\,2}$
3068.60686	5.16	$5_{2\,3}$	$5_{3\,2}$
3068.58802	16.90	$4_{1\,3}$	$4_{2\,2}$
3068.58527	6.58	$6_{5\,2}$	$6_{6\,1}$
3068.58247	61.35	$1_{1\,1}$	$2_{0\,2}$
3068.57736	10.68	$3_{0\,3}$	$3_{1\,2}$
3068.56818	18.46	$3_{1\,3}$	$3_{2\,2}$
3068.56434	33.02	$1_{0\,1}$	$2_{1\,2}$
3068.56126	8.38	$4_{2\,3}$	$4_{3\,2}$
3068.54939	9.04	$5_{3\,3}$	$5_{4\,2}$
3068.36807	56.44	$2_{1\,2}$	$3_{0\,3}$
3068.36613	35.23	$2_{0\,2}$	$3_{1\,3}$
3068.34170	38.23	$1_{1\,0}$	$2_{2\,1}$
3068.19493	15.23	$2_{2\,1}$	$3_{1\,2}$
3068.16712	26.04	$1_{1\,1}$	$2_{2\,0}$
3068.16119	69.32	$3_{1\,3}$	$4_{0\,4}$
		$3_{0\,3}$	$4_{1\,4}$
3068.15889	11.03	$5_{0\,5}$	$5_{1\,4}$
		$5_{1\,5}$	$5_{2\,4}$
3068.13623	33.80	$2_{1\,1}$	$3_{2\,2}$

3067.95956	16.81	$3_{2\,2}$	$4_{1\,3}$
3067.95389	52.05	$4_{1\,4}$	$5_{0\,5}$
		$4_{0\,4}$	$5_{1\,5}$
3067.94912	24.93	$3_{1\,2}$	$4_{2\,3}$
3067.90621	17.31	$2_{2\,0}$	$3_{3\,1}$
3067.82493	9.71	$3_{3\,1}$	$4_{2\,2}$
3067.76404	9.90	$2_{2\,1}$	$3_{3\,0}$
3067.74909	11.11	$4_{2\,3}$	$5_{1\,4}$
3067.74786	19.80	$4_{1\,3}$	$5_{2\,4}$
3067.74752	40.97	$5_{1\,5}$	$6_{0\,6}$
		$5_{0\,5}$	$6_{1\,6}$
3067.69814	8.42	$3_{2\,1}$	$4_{3\,2}$
3067.59069	3.75	$2_{1\,2}$	$3_{2\,1}$
3067.55656	9.23	$4_{3\,2}$	$5_{2\,3}$
3067.54165	23.64	$5_{2\,4}$	$6_{1\,5}$
		$5_{1\,4}$	$6_{2\,5}$
3067.54004	14.58	$6_{1\,6}$	$7_{0\,7}$
		$6_{0\,6}$	$7_{1\,7}$
3067.52496	6.23	$4_{2\,2}$	$5_{3\,3}$
3067.46382	14.78	$3_{3\,0}$	$4_{4\,1}$
3067.35911	15.31	$3_{3\,1}$	$4_{4\,0}$
3067.33628	9.32	$5_{3\,3}$	$6_{2\,4}$
3067.33349	14.27	$6_{2\,5}$	$7_{1\,6}$
		$6_{1\,5}$	$7_{2\,6}$
3067.33172	22.79	$7_{1\,7}$	$8_{0\,8}$
		$7_{0\,7}$	$8_{1\,8}$
3067.25256	8.21	$4_{3\,1}$	$5_{4\,2}$
3067.12785	13.89	$6_{2\,4}$	$7_{3\,5}$
3067.12604	11.87	$8_{0\,8}$	$9_{1\,9}$
		$8_{1\,8}$	$9_{0\,9}$
3067.08922	4.19	$5_{3\,2}$	$6_{4\,3}$
3067.02042	7.15	$4_{4\,0}$	$5_{5\,1}$
3066.94953	3.44	$4_{4\,1}$	$5_{5\,0}$
3066.82632	2.73	$4_{3\,2}$	$5_{4\,1}$
3066.79864	3.90	$5_{4\,1}$	$6_{5\,2}$
3066.57878	7.46	$5_{5\,0}$	$6_{6\,1}$
3066.44735	3.66	$5_{4\,2}$	$6_{5\,1}$
3066.34054	3.72	$6_{5\,1}$	$7_{6\,2}$

Table IV: Pyrazine transitions assigned to the minor band. The intensity is relative to the largest transition in the major band. The RMS deviation of the fit is 15 MHz.

Frequency (cm^{-1})	Intensity	$J'_{Ka'\,Kc'}$	$J''_{Ka''\,Kc''}$
3069.94042	4.75	$6_{5\,2}$	$5_{4\,1}$
3069.80463	3.18	$7_{3\,4}$	$6_{4\,3}$
3069.72557	7.74	$5_{5\,1}$	$4_{4\,0}$
3069.59617	6.40	$8_{2\,7}$	$7_{1\,6}$
		$8_{1\,7}$	$7_{2\,6}$
3069.58913	6.25	$9_{1\,9}$	$8_{0\,8}$
		$9_{0\,9}$	$8_{1\,8}$
3069.57548	3.96	$6_{3\,3}$	$5_{4\,2}$
3069.54262	4.59	$4_{3\,1}$	$3_{2\,2}$
3069.49348	3.99	$5_{4\,2}$	$4_{3\,1}$
3069.39642	7.91	$7_{2\,6}$	$6_{1\,5}$
		$7_{1\,6}$	$6_{2\,5}$
3069.39196	6.84	$4_{4\,0}$	$3_{3\,1}$
3069.39083	9.25	$8_{1\,8}$	$7_{0\,7}$
		$8_{0\,8}$	$7_{1\,7}$
3069.28717	5.22	$4_{4\,1}$	$3_{3\,0}$
3069.26544	3.30	$5_{3\,2}$	$4_{4\,1}$
3069.26493	4.24	$3_{3\,1}$	$2_{0\,2}$
3069.22081	6.66	$5_{3\,3}$	$4_{2\,2}$
3069.19860	10.41	$6_{2\,5}$	$5_{1\,4}$
		$6_{1\,5}$	$5_{2\,4}$
3069.19148	14.20	$7_{1\,7}$	$6_{0\,6}$
		$7_{0\,7}$	$6_{1\,6}$
3069.18780	3.28	$5_{2\,3}$	$4_{3\,2}$
3069.05201	6.39	$4_{3\,2}$	$3_{2\,1}$
3068.99801	6.82	$5_{2\,4}$	$4_{1\,3}$
3068.99681	7.67	$5_{1\,4}$	$4_{2\,3}$
3068.99125	20.57	$6_{1\,6}$	$5_{0\,5}$
		$6_{0\,6}$	$5_{1\,5}$
		$3_{3\,0}$	$2_{2\,1}$
3068.85008	18.76	$3_{3\,1}$	$2_{2\,0}$
3068.80147	7.10	$4_{2\,3}$	$3_{1\,2}$
3068.79145	30.74	$5_{1\,5}$	$4_{0\,4}$
		$5_{0\,5}$	$4_{1\,4}$
3068.79060	11.49	$4_{1\,3}$	$3_{2\,2}$

Frequency (cm^{-1})	Intensity	$J'_{Ka'\,Kc'}$	$J''_{Ka''\,Kc''}$
3068.78713	2.90	$6_{1\,5}$	$6_{0\,6}$
		$6_{2\,5}$	$6_{1\,6}$
3068.61895	8.17	$3_{2\,2}$	$2_{1\,1}$
3068.59056	9.08	$2_{2\,0}$	$1_{1\,1}$
3068.58968	30.42	$4_{1\,4}$	$3_{0\,3}$
		$4_{0\,4}$	$3_{1\,3}$
3068.58527	6.58	$5_{1\,4}$	$5_{0\,5}$
		$5_{2\,4}$	$5_{1\,5}$
3068.55451	12.22	$3_{1\,2}$	$2_{2\,1}$
3068.41641	14.36	$2_{2\,1}$	$1_{1\,0}$
3068.38887	34.78	$3_{1\,3}$	$2_{0\,2}$
3068.38688	19.28	$3_{0\,3}$	$2_{1\,2}$
3068.38520	4.41	$4_{2\,3}$	$4_{1\,4}$
3068.38367	4.70	$4_{1\,3}$	$4_{0\,4}$
3068.38031	4.32	$5_{3\,3}$	$5_{2\,4}$
3068.19303	23.62	$2_{1\,2}$	$1_{0\,1}$
3068.18794	4.43	$4_{3\,2}$	$4_{2\,3}$
3068.18551	5.91	$3_{2\,2}$	$3_{1\,3}$
3068.17425	13.25	$2_{0\,2}$	$1_{1\,1}$
3068.06262	3.38	$4_{4\,1}$	$4_{3\,2}$
3068.03037	7.87	$3_{3\,1}$	$3_{2\,2}$
3068.00661	6.42	$2_{2\,1}$	$2_{1\,2}$
3067.98980	23.35	$1_{1\,1}$	$0_{0\,0}$
3067.95552	12.31	$2_{1\,1}$	$2_{0\,2}$
3067.93868	7.12	$3_{2\,1}$	$3_{1\,2}$
3067.92438	10.57	$4_{3\,1}$	$4_{2\,2}$
3067.87514	4.17	$4_{4\,0}$	$4_{3\,1}$
3067.83019	9.59	$3_{3\,0}$	$3_{2\,1}$
3067.80133	11.54	$2_{2\,0}$	$2_{1\,1}$
3067.78459	20.96	$1_{1\,0}$	$1_{0\,1}$
3067.56152	9.59	$1_{0\,1}$	$1_{1\,0}$
3067.54165	23.64	$2_{1\,1}$	$2_{2\,0}$
3067.50752	6.80	$3_{2\,1}$	$3_{3\,0}$
3067.45724	5.84	$4_{3\,1}$	$4_{4\,0}$

3067.38491	5.95	$2_{0\,2}$	$2_{1\,1}$
3067.35760	10.24	$0_{0\,0}$	$1_{1\,1}$
3067.33696	6.92	$2_{1\,2}$	$2_{2\,1}$
3067.30956	2.77	$3_{2\,2}$	$3_{3\,1}$
3067.27213	3.39	$4_{3\,2}$	$4_{4\,1}$
3067.17229	4.39	$4_{1\,3}$	$4_{2\,2}$
3067.16976	17.37	$1_{1\,1}$	$2_{0\,2}$
3067.16292	4.62	$3_{0\,3}$	$3_{1\,2}$
3067.15330	4.36	$3_{1\,3}$	$3_{2\,2}$
3067.15148	11.82	$1_{0\,1}$	$2_{1\,2}$
3067.14523	3.17	$4_{2\,3}$	$4_{3\,2}$
3067.13113	2.91	$5_{3\,3}$	$5_{4\,2}$
3067.11231	4.28	$6_{4\,3}$	$6_{5\,2}$
3066.95366	14.40	$2_{1\,2}$	$3_{0\,3}$
3066.95100	8.77	$2_{0\,2}$	$3_{1\,3}$
3066.92812	10.06	$1_{1\,0}$	$2_{2\,1}$
3066.78093	4.70	$2_{2\,1}$	$3_{1\,2}$
3066.75350	5.84	$1_{1\,1}$	$2_{2\,0}$
3066.74516	18.65	$3_{1\,3}$	$4_{0\,4}$
		$3_{0\,3}$	$4_{1\,4}$
3066.73936	3.33	$5_{0\,5}$	$5_{1\,4}$
		$5_{1\,5}$	$5_{2\,4}$
3066.71977	7.52	$2_{1\,1}$	$3_{2\,2}$
3066.54460	5.45	$3_{2\,2}$	$4_{1\,3}$

3066.53634	13.31	$4_{1\,4}$	$5_{0\,5}$
		$4_{0\,4}$	$5_{1\,5}$
3066.53257	7.93	$3_{1\,2}$	$4_{2\,3}$
3066.49195	3.43	$2_{2\,0}$	$3_{3\,1}$
3066.41449	3.24	$3_{3\,1}$	$4_{2\,2}$
3066.35003	3.96	$2_{2\,1}$	$3_{3\,0}$
3066.33235	3.32	$4_{2\,3}$	$5_{1\,4}$
3066.33136	4.97	$4_{1\,3}$	$5_{2\,4}$
3066.32830	13.62	$5_{1\,5}$	$6_{0\,6}$
		$5_{0\,5}$	$6_{1\,6}$
3066.28139	5.75	$3_{2\,1}$	$4_{3\,2}$
3066.14095	3.65	$4_{3\,2}$	$5_{2\,3}$
3066.12313	5.29	$5_{2\,4}$	$6_{1\,5}$
		$5_{1\,4}$	$6_{2\,5}$
3066.11780	8.35	$6_{1\,6}$	$7_{0\,7}$
		$6_{0\,6}$	$7_{1\,7}$
3066.11270	4.11	$4_{2\,2}$	$5_{3\,3}$
3066.04937	4.69	$3_{3\,0}$	$4_{4\,1}$
3065.94434	7.63	$3_{3\,1}$	$4_{4\,0}$
3065.91914	3.46	$5_{3\,3}$	$6_{2\,4}$
3065.91442	3.92	$5_{2\,3}$	$6_{3\,4}$
3065.91358	6.42	$6_{2\,5}$	$7_{1\,6}$
		$6_{1\,5}$	$7_{2\,6}$
3065.90744	6.65	$7_{1\,7}$	$8_{0\,8}$
		$7_{0\,7}$	$8_{1\,8}$

Table V: The table presents the experimental transitions in naphthalene which are fragmented as a result of mode coupling, and the coupling matrix elements. Three distinct excited state transitions are fragmented and have an average coupling matrix element of 0.0016 cm^{-1}.

Excited State	Ground State	Frequency (cm^{-1})	<L | H' | D> (cm^{-1})
6_{06}	5_{15}	3064.94772 3064.95018	0.0013
6_{06}	7_{17}	3064.12841 3064.13129	0.0013
6_{16}	5_{05}	3064.97471 3064.97971	0.0022
6_{16}	7_{07}	3064.14386 3064.14788	0.0022
9_{09}	8_{18}	3065.13418 3065.13658	0.0012
9_{09}	$10_{1\,10}$	3063.95668 3063.95926	0.0012

Table VI: The transitions in naphthalene which deviate significantly more than experimental uncertainty from the calculated transitions. The frequency and residuals given in cm^{-1}.

$J'\ K_a'\ K_c'$	$J''\ K_a''\ K_c''$	Frequency	Residuals
6_{51}	5_{42}	3065.6275	0.0017
	6_{42}	3065.1991	0.0021
	7_{62}	3063.3361	0.0024
6_{52}	5_{41}	3065.6275	0.0018
	6_{43}	3065.1991	0.0017
	7_{61}	3063.3361	0.0024
6_{60}	5_{51}	3065.7697	0.0060
	6_{51}	3065.3427	0.0061
	7_{71}	3063.2027	0.0048
6_{61}	5_{50}	3065.7697	0.0060
	6_{52}	3065.3427	0.0061
	7_{70}	3063.2027	0.0048
7_{52}	6_{43}	3065.6986	0.0023
	7_{43}	3065.1955	0.0015
	8_{63}	3063.2644	0.0020
7_{53}	6_{42}	3065.6983	0.0024
	7_{44}	3065.1980	0.0028
	7_{62}	3063.8339	0.0013
	8_{62}	3063.2644	0.0020
7_{61}	6_{52}	3065.8405	0.0061
	7_{52}	3065.3410	0.0059
	8_{72}	3063.1316	0.0052
7_{62}	6_{51}	3065.8405	0.0061
	7_{53}	3065.3410	0.0059
	8_{71}	3063.1316	0.0052
8_{53}	7_{44}	3065.7697	0.0030
	8_{44}	3065.1911	0.0020
	8_{62}	3063.8353	0.0014
	9_{64}	3063.1930	0.0017
8_{54}	7_{43}	3065.7679	0.0026
	8_{45}	3065.1939	0.0013
	8_{63}	3063.8353	0.0016
	9_{63}	3063.1930	0.0018
8_{62}	7_{53}	3065.9109	0.0061
	8_{53}	3065.3389	0.0061
	9_{73}	3063.0604	0.0054
8_{63}	7_{52}	3065.9109	0.0062
	8_{54}	3065.3389	0.0060
	9_{72}	3063.0604	0.0054
8_{71}	7_{62}	3066.0399	-0.0031
	8_{62}	3065.4699	-0.0030
8_{72}	7_{51}	3066.0399	-0.0031
	8_{63}	3065.4699	-0.0030
9_{72}	8_{63}	3066.1104	-0.0030
	9_{63}	3065.4677	-0.0033
9_{73}	8_{62}	3066.1104	-0.0030
	9_{64}	3065.4677	-0.0033
11_{48}	10_{37}	3065.7458	0.0021
	11_{57}	3063.9771	0.0020
11_{57}	10_{46}	3065.9612	0.0022
	11_{66}	3063.8423	0.0014
12_{49}	11_{38}	3065.7730	0.0029
	$12_{3\,10}$	3065.1201	0.0023
$13_{4\,10}$	12_{39}	3065.7930	0.0027
	$13_{3\,11}$	3065.1493	0.0027
$18_{0\,18}$	$17_{1\,17}$	3065.6520	-0.0011
	$19_{1\,19}$	3063.4121	-0.0014
$18_{1\,18}$	$17_{0\,17}$	3065.6520	-0.0011
	$19_{0\,19}$	3063.4121	-0.0014
$18_{2\,16}$	$17_{3\,15}$	3065.7784	0.0030
	$18_{1\,17}$	3065.4703	0.0028
	$18_{3\,15}$	3063.8072	0.0019
	$19_{3\,17}$	3063.3004	0.0019

$18_{3\,16}$	$17_{2\,15}$	3065.7858	0.0013
	$18_{4\,15}$	3063.7719	0.0015
$19_{0\,19}$	$18_{1\,18}$	3065.7200	0.0103
	$20_{1\,20}$	3063.3630	0.0108
$19_{1\,18}$	$18_{2\,17}$	3065.7753	0.0027
	$20_{2\,19}$	3063.2986	0.0018
$19_{1\,19}$	$18_{0\,18}$	3065.7200	0.0103
	$20_{0\,20}$	3063.3630	0.0108
$19_{2\,18}$	$18_{1\,17}$	3065.7755	0.0027
	$20_{1\,19}$	3063.2986	0.0017
$20_{0\,20}$	$19_{1\,19}$	3065.7721	0.0058
	$21_{1\,21}$	3063.2963	0.0054
$20_{1\,19}$	$19_{2\,18}$	3065.8261	-0.0033
	$21_{2\,20}$	3063.2330	-0.0027
$20_{1\,20}$	$19_{0\,19}$	3065.7721	0.0058
	$21_{0\,21}$	3063.2963	0.0054
$20_{2\,19}$	$19_{1\,18}$	3065.8261	-0.0034
	$21_{1\,20}$	3063.2330	-0.0028
$22_{0\,22}$	$21_{1\,21}$	3065.8809	0.0020
	$23_{1\,23}$	3063.1702	0.0024
$22_{1\,22}$	$21_{0\,21}$	3065.8809	0.0020
	$23_{0\,23}$	3063.1702	0.0024

Table VII: The assignments for the transitions in the naphthalene spectrum. The intensity is relative to the largest experimental transition. Transitions marked with a (‡) were not used in the final fit. The RMS deviation of the fit is 19 MHz.

Frequency (cm^{-1})	Intensity	$J'_{K_a' K_c'}$	$J''_{K_a'' K_c''}$
3066.39036	55.4	9_{91}	8_{80}
		9_{90}	8_{81}
3066.32277	41.2	10_{82}	9_{73}
		10_{83}	9_{72}
3066.25319	61.7	11_{75}	10_{64}
		11_{74}	10_{65}
3066.24955	54.6	9_{81}	8_{72}
		9_{82}	8_{71}
3066.18328	73.0	12_{66}	11_{57}
		10_{74}	9_{63}
		10_{73}	9_{64}
3066.17971	72.6	8_{81}	7_{70}
		8_{80}	7_{71}
3066.14407	11.0	13_{58}	12_{49}
3066.12787	16.0	16_{512}	15_{411}
3066.11461	9.0	11_{65}	10_{56}
3066.11090	14.7	25_{224}	24_{123}
		25_{124}	24_{223}
‡3066.11042	55.7	9_{72}	8_{63}
		9_{73}	8_{62}
3066.08880	11.0	14_{510}	13_{49}
3066.06228	18.7	23_{321}	22_{220}
		23_{221}	22_{320}
3066.05927	20.8	12_{57}	11_{48}
‡3066.03990 ‡	68.7	8_{71}	7_{62}
		8_{72}	7_{61}
3065.98989	20.6	24_{124}	23_{023}
		24_{024}	23_{123}
‡3065.96115	13.3	11_{57}	10_{46}
3065.95000	14.3	21_{319}	20_{218}
3065.94234	28.7	22_{221}	21_{120}
		22_{121}	21_{220}
3065.93489	27.4	23_{123}	22_{022}
		23_{023}	22_{122}
‡3065.91090 ‡	50.9	8_{62}	7_{53}
		8_{63}	7_{52}
3065.89512	14.8	18_{415}	17_{314}
		20_{318}	19_{217}
3065.89282	37.4	20_{218}	19_{317}
‡3065.88086 ‡	49.4	22_{022}	21_{121}
		22_{122}	21_{021}
‡3065.84046 ‡	55.4	7_{61}	6_{52}
		7_{62}	6_{51}
3065.83923	25.2	19_{317}	18_{216}
3065.83743	11.2	9_{54}	8_{45}
3065.83311	16.1	9_{55}	8_{44}
‡3065.82608 ‡	40.6	20_{119}	19_{218}
		20_{219}	19_{118}
3065.82201	38.0	21_{121}	20_{020}
		21_{021}	20_{120}
		15_{412}	14_{311}
3065.80966	20.7	10_{46}	9_{37}
3065.80545	16.4	14_{411}	13_{310}
3065.79850	10.8	18_{315}	17_{414}
‡3065.79295	8.6	13_{410}	12_{39}
‡3065.78581	10.3	18_{316}	17_{215}
‡3065.77839	25.1	18_{216}	17_{315}
‡3065.77553	38.6	19_{218}	18_{117}
‡3065.77529	27.5	19_{118}	18_{217}
‡3065.77295	15.2	12_{49}	11_{38}
‡3065.77206 ‡	41.5	20_{020}	19_{119}
		20_{120}	19_{019}
‡3065.76969 ‡ ‡	60.7	6_{60}	5_{51}
		6_{61}	5_{50}
		8_{53}	7_{44}
‡3065.76793	22.2	8_{54}	7_{43}
‡3065.74579	14.0	11_{48}	10_{37}
‡3065.72002 ‡	45.1	19_{019}	18_{118}
		19_{119}	18_{018}
3065.73140	29.2	17_{315}	16_{214}

3065.71695	30.6	$18_{2\,17}$	$17_{1\,16}$
		$18_{1\,17}$	$17_{2\,16}$
		$17_{3\,14}$	$16_{4\,13}$
3065.71536	21.3	$17_{2\,15}$	$16_{3\,14}$
‡3065.69862	25.0	$7_{5\,2}$	$6_{4\,3}$
‡3065.69828	33.7	$7_{5\,3}$	$6_{4\,2}$
3065.68148	15.5	$16_{3\,14}$	$15_{2\,13}$
3065.65197	62.8	$16_{2\,14}$	$15_{3\,13}$
‡		$18_{0\,18}$	$17_{1\,17}$
‡		$18_{1\,18}$	$17_{0\,17}$
3065.63691	11.9	$8_{4\,4}$	$7_{3\,5}$
3065.63325	13.3	$15_{3\,13}$	$14_{2\,12}$
‡3065.62752	27.1	$6_{5\,1}$	$5_{4\,2}$
‡		$6_{5\,2}$	$5_{4\,1}$
3065.61202	20.6	$8_{4\,5}$	$7_{3\,4}$
3065.60953	20.3	$10_{8\,3}$	$10_{7\,4}$
		$10_{8\,2}$	$10_{7\,3}$
3065.60393	22.7	$12_{8\,5}$	$12_{7\,6}$
		$12_{8\,4}$	$12_{7\,5}$
3065.60298	23.6	$16_{2\,15}$	$15_{1\,14}$
3065.60180	43.0	$16_{1\,15}$	$15_{2\,14}$
3065.59682	78.0	$17_{0\,17}$	$16_{1\,16}$
		$17_{1\,17}$	$16_{0\,16}$
3065.58541	22.9	$15_{2\,13}$	$14_{3\,12}$
3065.55654	42.5	$5_{5\,1}$	$4_{4\,0}$
		$5_{5\,0}$	$4_{4\,1}$
3065.55348	28.6	$13_{3\,11}$	$12_{2\,10}$
3065.55123	17.9	$7_{4\,4}$	$6_{3\,3}$
3065.54652	32.6	$15_{2\,14}$	$14_{1\,13}$
3065.54383	25.3	$15_{1\,14}$	$14_{2\,13}$
3065.54040	86.7	$16_{0\,16}$	$15_{1\,15}$
		$16_{1\,16}$	$15_{0\,15}$
3065.51440	25.6	$14_{2\,12}$	$13_{3\,11}$
3065.49199	15.4	$14_{2\,13}$	$13_{1\,12}$
3065.48448	29.1	$6_{4\,3}$	$5_{3\,2}$
3065.48409	24.0	$14_{1\,13}$	$13_{2\,12}$
		$20_{4\,17}$	$20_{3\,18}$
3065.48243	100.0	$15_{0\,15}$	$14_{1\,14}$
		$15_{1\,15}$	$14_{0\,14}$
3065.47298	9.1	$20_{3\,17}$	$20_{2\,18}$
‡3065.46989	28.5	$18_{2\,16}$	$18_{1\,17}$
‡		$8_{7\,1}$	$8_{6\,2}$
‡		$8_{7\,2}$	$8_{6\,3}$
3065.46901	23.8	$10_{7\,4}$	$10_{6\,5}$
		$10_{7\,3}$	$10_{6\,4}$
‡3065.46765	28.3	$9_{7\,2}$	$9_{6\,3}$
‡		$9_{7\,3}$	$9_{6\,4}$
3065.46490	21.5	$11_{7\,5}$	$11_{6\,6}$
		$11_{7\,4}$	$11_{6\,5}$
3065.45671	15.8	$13_{7\,7}$	$13_{6\,8}$
3065.43597	30.3	$13_{2\,12}$	$12_{1\,11}$
3065.43583	31.7	$13_{2\,11}$	$12_{3\,10}$
3065.43032	15.9	$17_{7\,11}$	$17_{6\,12}$
3065.42610	88.0	$14_{0\,14}$	$13_{1\,13}$
		$14_{1\,14}$	$13_{0\,13}$
3065.42503	26.8	$13_{1\,12}$	$12_{2\,11}$
3065.41827	20.2	$5_{4\,1}$	$4_{3\,2}$
3065.41654	20.1	$5_{4\,2}$	$4_{3\,1}$
3065.40828	18.3	$17_{2\,15}$	$17_{1\,16}$
		$14_{3\,11}$	$13_{4\,10}$
3065.40513	16.4	$19_{3\,16}$	$19_{2\,17}$
		$8_{3\,6}$	$7_{2\,5}$
3065.37503	24.5	$6_{3\,3}$	$5_{2\,4}$
3065.37107	15.5	$18_{4\,15}$	$18_{3\,16}$
3065.36855	58.7	$13_{1\,13}$	$12_{0\,12}$
3065.36781	43.6	$13_{0\,13}$	$12_{1\,12}$
3065.36391	40.5	$12_{1\,11}$	$11_{2\,10}$
3065.34804	18.3	$12_{2\,10}$	$11_{3\,9}$
3065.34733	14.0	$4_{4\,1}$	$3_{3\,0}$
		$4_{4\,0}$	$3_{3\,1}$
3065.34512	11.8	$16_{2\,14}$	$16_{1\,15}$
‡3065.34269	13.4	$6_{6\,0}$	$6_{5\,1}$
‡		$6_{6\,1}$	$6_{5\,2}$
‡3065.34097	25.8	$7_{6\,1}$	$7_{5\,2}$
‡		$7_{6\,2}$	$7_{5\,3}$
‡3065.33891	28.8	$8_{6\,2}$	$8_{5\,3}$
‡		$8_{6\,3}$	$8_{5\,4}$

3065.33663	15.2	$14_{2\,13}$	$14_{1\,14}$
3065.33420	18.1	$14_{1\,13}$	$14_{0\,14}$
3065.33244	34.7	$11_{2\,10}$	$10_{1\,9}$
3065.32267	12.5	$11_{6\,6}$	$11_{5\,7}$
3065.32132	14.2	$6_{3\,4}$	$5_{2\,3}$
3065.31970	14.4	$17_{4\,14}$	$17_{3\,15}$
		$11_{6\,5}$	$11_{5\,6}$
		$18_{6\,13}$	$18_{5\,14}$
3065.31102	37.4	$12_{1\,12}$	$11_{0\,11}$
3065.31028	42.9	$12_{0\,12}$	$11_{1\,11}$
3065.30720	14.2	$16_{6\,11}$	$16_{5\,12}$
		$15_{6\,10}$	$15_{5\,11}$
3065.30005	29.6	$11_{1\,10}$	$10_{2\,9}$
		$20_{4\,16}$	$20_{3\,17}$
3065.29747	13.3	$13_{6\,7}$	$13_{5\,8}$
3065.29107	27.1	$5_{3\,2}$	$4_{2\,3}$
3065.28485	32.6	$10_{2\,9}$	$9_{1\,8}$
3065.26874	8.7	$16_{4\,13}$	$16_{3\,14}$
		$17_{5\,13}$	$17_{4\,14}$
3065.26674	30.6	$5_{3\,3}$	$4_{2\,2}$
3065.25333	60.0	$11_{1\,11}$	$10_{0\,10}$
3065.25220	54.2	$11_{0\,11}$	$10_{1\,10}$
3065.25169	19.0	$11_{2\,9}$	$10_{3\,8}$
3065.24320	14.4	$5_{2\,3}$	$4_{1\,4}$
3065.24072	20.9	$9_{2\,8}$	$8_{1\,7}$
3065.23124	39.2	$10_{1\,9}$	$9_{2\,8}$
3065.22304	14.7	$15_{4\,12}$	$15_{3\,13}$
3065.22053	13.8	$12_{2\,11}$	$12_{1\,12}$
		$16_{6\,10}$	$16_{5\,11}$
3065.21742	14.6	$19_{4\,15}$	$19_{3\,16}$
		$15_{5\,11}$	$15_{4\,12}$
3065.21657	20.4	$14_{2\,12}$	$14_{1\,13}$
3065.21394	23.7	$12_{1\,11}$	$12_{0\,12}$
3065.21278	13.2	$4_{3\,1}$	$3_{2\,2}$
3065.20528	10.6	$4_{3\,2}$	$3_{2\,1}$
3065.20202	18.8	$8_{2\,7}$	$7_{1\,6}$
‡3065.19913	17.4	$6_{5\,1}$	$6_{4\,2}$
‡		$6_{5\,2}$	$6_{4\,3}$
‡3065.19804	20.6	$7_{5\,3}$	$7_{4\,4}$
3065.19658	17.8	$10_{1\,10}$	$9_{0\,9}$
‡3065.19551	39.5	$7_{5\,2}$	$7_{4\,3}$
3065.19392	54.2	$10_{0\,10}$	$9_{1\,9}$
‡		$8_{5\,4}$	$8_{4\,5}$
3065.19213	26.6	$13_{5\,9}$	$13_{4\,10}$
‡3065.19112	19.3	$8_{5\,3}$	$8_{4\,4}$
3065.19092	23.3	$13_{3\,11}$	$13_{2\,12}$
3065.19003	31.7	$16_{3\,13}$	$16_{2\,14}$
		$9_{5\,5}$	$9_{4\,6}$
3065.18153	20.4	$14_{4\,11}$	$14_{3\,12}$
3065.16513	18.8	$11_{2\,10}$	$11_{1\,11}$
3065.16470	24.7	$7_{2\,6}$	$6_{1\,5}$
3065.15672	18.5	$9_{1\,8}$	$8_{2\,7}$
3065.15381	16.1	$11_{1\,10}$	$11_{0\,11}$
3065.14933	17.6	$10_{2\,8}$	$9_{3\,7}$
‡		$13_{4\,10}$	$13_{3\,11}$
3065.14850	23.1	$13_{2\,11}$	$13_{1\,12}$
3065.14099	42.5	$9_{1\,9}$	$8_{0\,8}$
3065.13851	33.5	$3_{3\,0}$	$2_{2\,1}$
3065.13752	23.9	$3_{3\,1}$	$2_{2\,0}$
		$18_{4\,14}$	$18_{3\,15}$
‡3065.13658	16.5	$9_{0\,9}$	$8_{1\,8}$
‡3065.13418	25.5	$9_{0\,9}$	$8_{1\,8}$
3065.12457	25.0	$6_{2\,5}$	$5_{1\,4}$
		$12_{5\,7}$	$12_{4\,8}$
‡3065.12010	17.8	$12_{4\,9}$	$12_{3\,10}$
3065.11142	12.8	$15_{3\,12}$	$15_{2\,13}$
3065.11014	19.6	$10_{2\,9}$	$10_{1\,10}$
3065.09245	30.6	$13_{5\,8}$	$13_{4\,9}$
3065.09034	24.0	$10_{1\,9}$	$10_{0\,10}$
3065.08504	48.6	$8_{1\,8}$	$7_{0\,7}$
3065.08254	14.8	$20_{6\,14}$	$20_{5\,15}$
		$5_{2\,4}$	$4_{1\,3}$
3065.07669	51.3	$12_{2\,10}$	$12_{1\,11}$
		$8_{1\,7}$	$7_{2\,6}$
3065.07602	26.7	$8_{0\,8}$	$7_{1\,7}$

3065.06992	24.5	9_{46}	9_{37}
3065.06335	21.3	17_{413}	17_{314}
3065.06289	22.6	8_{45}	8_{36}
3065.05857	29.5	5_{41}	5_{32}
3065.05666	24.5	9_{28}	9_{19}
3065.05349	14.7	10_{38}	10_{29}
3065.03782	13.6	14_{311}	14_{212}
3065.03560	31.6	4_{23}	3_{12}
3065.02956	25.2	7_{17}	6_{06}
3065.02498	19.8	3_{21}	2_{12}
		9_{18}	9_{09}
3065.01402	19.1	7_{07}	6_{16}
3065.00586	12.6	8_{27}	8_{18}
3065.00186	21.4	16_{412}	16_{313}
3064.99778	15.2	9_{45}	9_{36}
3064.98938	24.1	7_{16}	6_{25}
3064.98745	20.8	8_{36}	8_{27}
3064.98353	16.0	3_{22}	2_{11}
‡3064.97971	21.9	6_{16}	5_{05}
‡3064.97471	23.6	6_{16}	5_{05}
3064.97361	27.4	10_{46}	10_{37}
3064.96801	22.3	13_{310}	13_{211}
3064.96538	21.6	7_{35}	7_{26}
3064.95917	33.8	7_{26}	7_{17}
3064.95757	17.3	8_{17}	8_{08}
		15_{411}	15_{312}
‡3064.95018	10.7	6_{06}	5_{15}
3064.94850	16.8	6_{34}	6_{25}
‡3064.94772	21.1	6_{06}	5_{15}
3064.94662	24.6	11_{47}	11_{38}
3064.93779	22.6	5_{33}	5_{24}
3064.93667	15.3	2_{20}	1_{11}
3064.93362	12.8	8_{26}	7_{35}
		10_{28}	10_{19}
3064.93119	20.7	4_{32}	4_{23}
		14_{410}	14_{311}
3064.92765	27.7	12_{48}	12_{39}
3064.92672	41.2	3_{31}	3_{22}
		5_{15}	4_{04}
3064.92375	23.8	2_{21}	1_{10}
3064.92031	11.0	3_{30}	3_{21}
3064.91645	15.2	6_{25}	6_{16}
3064.91258	24.7	12_{39}	12_{210}
3064.91190	17.7	4_{31}	4_{22}
3064.89785	21.4	6_{15}	5_{24}
3064.89637	22.3	5_{32}	5_{23}
3064.89034	18.5	7_{16}	7_{07}
3064.88202	22.3	5_{05}	4_{14}
3064.87915	10.2	5_{24}	5_{15}
3064.87819	25.3	4_{14}	3_{03}
3064.87767	26.7	6_{33}	6_{24}
3064.87359	11.0	11_{38}	11_{29}
3064.87248	22.4	9_{27}	9_{18}
3064.85799	31.2	7_{34}	7_{25}
3064.84981	43.2	10_{37}	10_{28}
3064.84898	16.3	4_{23}	4_{14}
3064.84245	29.5	8_{35}	8_{26}
3064.84092	19.6	9_{36}	9_{27}
3064.82727	24.3	7_{25}	6_{34}
		3_{13}	2_{02}
3064.82615	23.0	6_{15}	6_{06}
3064.82450	14.6	3_{22}	3_{13}
3064.82184	23.7	8_{26}	8_{17}
3064.80996	24.8	4_{04}	3_{13}
3064.78508	29.4	7_{25}	7_{16}
3064.77474	23.0	2_{12}	1_{01}
3064.77287	15.9	2_{20}	2_{11}
3064.77056	27.9	5_{14}	5_{05}
3064.76341	28.4	6_{24}	6_{15}
3064.76248	21.8	3_{21}	3_{12}
3064.75418	31.3	4_{22}	4_{13}
3064.75362	26.0	5_{23}	5_{14}
3064.73469	15.8	3_{03}	2_{12}

3064.72512	33.3	6_{24}	5_{33}
		4_{13}	4_{04}
3064.71579	16.4	1_{11}	0_{00}
3064.69194	23.1	3_{12}	3_{03}
3064.66985	27.6	2_{11}	2_{02}
3064.65709	20.2	1_{10}	1_{01}
3064.50694	17.4	1_{01}	1_{10}
3064.49434	19.3	2_{02}	2_{11}
3064.47178	22.3	3_{03}	3_{12}
3064.43818	23.6	4_{04}	4_{13}
3064.42876	11.2	2_{12}	3_{03}
3064.41056	47.3	4_{13}	4_{22}
		5_{14}	5_{23}
3064.40281	17.9	3_{12}	3_{21}
3064.39987	32.1	6_{15}	6_{24}
3064.39161	39.2	5_{05}	5_{14}
		2_{11}	2_{20}
3064.38949	12.3	1_{01}	2_{12}
3064.37634	27.3	7_{16}	7_{25}
3064.35897	18.2	4_{23}	5_{14}
		2_{12}	2_{21}
3064.35291	24.8	3_{13}	4_{04}
3064.33940	30.1	8_{17}	8_{26}
		3_{13}	3_{22}
3064.32216	30.6	9_{27}	9_{36}
3064.31845	19.6	8_{26}	8_{35}
3064.31510	22.8	4_{14}	4_{23}
3064.31182	14.3	10_{28}	10_{37}
3064.30464	23.3	7_{25}	7_{34}
3064.28745	10.4	9_{18}	9_{27}
3064.28636	19.2	6_{24}	6_{33}
		11_{29}	11_{38}
3064.28482	34.7	3_{03}	4_{14}
3064.28288	14.4	5_{15}	5_{24}
3064.28029	27.4	4_{14}	5_{05}
3064.26996	5.4	7_{07}	7_{16}
3064.26840	15.7	5_{23}	5_{32}
3064.25393	8.0	4_{22}	4_{31}
3064.24549	17.7	12_{210}	12_{39}
		3_{21}	3_{30}
3064.24100	18.5	1_{10}	2_{21}
3064.23533	25.7	4_{04}	5_{15}
3064.23440	14.1	4_{23}	4_{32}
3064.23154	17.8	12_{39}	12_{48}
3064.22903	21.0	14_{311}	14_{410}
		1_{11}	2_{20}
3064.22443	26.4	10_{19}	10_{28}
3064.21573	8.2	11_{38}	11_{47}
3064.21431	12.5	6_{25}	6_{34}
3064.21202	50.1	5_{15}	6_{06}
3064.20258	8.2	7_{17}	7_{26}
3064.20133	5.0	8_{08}	8_{17}
3064.19735	10.7	7_{26}	7_{35}
3064.19115	25.6	10_{37}	10_{46}
3064.18865	17.3	13_{211}	13_{310}
3064.18390	25.1	5_{05}	6_{16}
3064.18218	12.4	2_{11}	3_{22}
3064.17230	12.9	8_{27}	8_{36}
		6_{25}	7_{16}
3064.16319	11.4	9_{36}	9_{45}
3064.15312	29.2	8_{18}	8_{27}
		16_{313}	16_{412}
		11_{110}	11_{29}
‡3064.14788	19.7	6_{16}	7_{07}
‡3064.14386	11.2	6_{16}	7_{07}
3064.13972	10.0	2_{12}	3_{21}
‡3064.13129	16.5	6_{06}	7_{17}
3064.12872	23.5	3_{12}	4_{23}
‡3064.12841	28.3	6_{06}	7_{17}
3064.11798	24.9	14_{212}	14_{311}
3064.11352	26.1	6_{33}	6_{42}
3064.11319	10.3	19_{415}	19_{514}
3064.10822	11.2	5_{32}	5_{41}

3064.10530	14.4	10_{29}	10_{38}
		6_{34}	6_{43}
		5_{33}	5_{42}
3064.10486	17.6	7_{35}	7_{44}
3064.09290	14.4	9_{37}	9_{46}
3064.08302	21.0	7_{17}	8_{08}
3064.08164	22.1	4_{13}	5_{24}
		10_{38}	10_{47}
3064.07920	26.5	12_{111}	12_{210}
3064.07417	10.8	7_{07}	8_{18}
3064.06708	7.6	13_{49}	13_{58}
3064.06413	10.2	11_{39}	11_{48}
		22_{517}	22_{616}
3064.06114	17.9	11_{210}	11_{39}
3064.03998	10.3	12_{310}	12_{49}
		15_{213}	15_{312}
3064.03742	17.1	3_{13}	4_{22}
		5_{14}	6_{25}
3064.02791	15.7	2_{20}	3_{31}
3064.02637	12.0	2_{21}	3_{30}
3064.02143	27.2	8_{18}	9_{09}
3064.01733	25.4	8_{08}	9_{19}
3064.01384	13.3	12_{211}	12_{310}
3064.01284	10.9	11_{47}	11_{56}
3064.01121	13.2	9_{37}	10_{28}
3064.00855	19.6	13_{311}	13_{410}
3064.00466	11.4	13_{112}	13_{211}
3064.00180	10.9	8_{27}	9_{18}
3063.99945	12.1	11_{011}	11_{110}
3063.99827	19.2	6_{15}	7_{26}
3063.99528	10.3	10_{46}	10_{55}
3063.98804	12.5	11_{111}	11_{210}
‡3063.97712	15.0	11_{48}	11_{57}
3063.97413	20..2	9_{46}	9_{55}
3063.97000	17.3	6_{43}	6_{52}
		6_{42}	6_{51}
3063.96125	37.2	3_{21}	4_{32}
		13_{212}	13_{311}
3063.95996	20.8	9_{19}	10_{010}
		7_{16}	8_{27}
		16_{214}	16_{313}
‡3063.95926	14.5	9_{09}	10_{110}
‡3063.95668	22.1	9_{09}	10_{110}
3063.95297	14.0	3_{22}	4_{31}
3063.92640	24.6	9_{28}	10_{19}
3063.91729	20.9	8_{17}	9_{28}
3063.89945	12.3	10_{110}	11_{011}
3063.89785	44.9	10_{010}	11_{111}
		4_{22}	5_{33}
3063.88379	8.3	17_{414}	17_{513}
3063.88142	18.9	17_{215}	17_{314}
		14_{59}	14_{68}
3063.87976	13.5	16_{314}	16_{413}
3063.87409	12.6	4_{23}	5_{32}
3063.87340	8.8	9_{18}	10_{29}
3063.86533	8.2	15_{114}	15_{213}
3063.85733	18.6	10_{29}	11_{110}
3063.84703	15.1	15_{214}	15_{313}
3063.84235 ‡	27.4	5_{23}	6_{34}
		11_{57}	11_{66}
3063.83862	31.7	11_{111}	12_{012}
‡3063.83386	12.9	7_{53}	7_{62}
3063.83801	41.6	11_{011}	12_{112}
‡3063.83527 ‡	14.8	8_{53}	8_{62}
		8_{54}	8_{63}
3063.82443	24.0	10_{19}	11_{210}
3063.82032	34.1	3_{30}	4_{41}
		3_{31}	4_{40}
‡3063.80720	15.5	18_{216}	18_{315}
3063.79057	24.0	11_{210}	12_{111}
3063.77802	35.1	12_{012}	13_{113}
		12_{112}	13_{013}
3063.77186 ‡	19.7	11_{110}	12_{211}
		18_{316}	18_{415}
3063.75618	3.4	7_{25}	8_{36}
3063.75023	8.5	13_{410}	14_{311}

3063.74947	13.4	$4_{3\,1}$	$5_{4\,2}$
3063.74883	20.4	$4_{3\,2}$	$5_{4\,1}$
3063.72159	19.0	$8_{2\,6}$	$9_{3\,7}$
3063.71786	41.0	$13_{1\,13}$	$14_{0\,14}$
3063.71729	23.1	$13_{0\,13}$	$14_{1\,14}$
3063.71615	13.5	$15_{6\,10}$	$15_{7\,9}$
3063.71535	23.1	$12_{1\,11}$	$13_{2\,12}$
3063.69282	9.7	$9_{2\,7}$	$10_{3\,8}$
		$6_{2\,5}$	$7_{3\,4}$
3063.67999	12.9	$5_{3\,2}$	$6_{4\,3}$
3063.67658	24.5	$5_{3\,3}$	$6_{4\,2}$
3063.66301	16.5	$13_{2\,12}$	$14_{1\,13}$
3063.65754	47.0	$14_{1\,14}$	$15_{0\,15}$
		$14_{0\,14}$	$15_{1\,15}$
3063.63923	12.4	$13_{3\,11}$	$14_{2\,12}$
3063.61299	26.1	$4_{4\,1}$	$5_{5\,0}$
		$4_{4\,0}$	$5_{5\,1}$
3063.60195	10.9	$6_{3\,4}$	$7_{4\,3}$
3063.60121	7.7	$12_{2\,10}$	$13_{3\,11}$
3063.59911	23.1	$14_{1\,13}$	$15_{2\,14}$
3063.56201	4.1	$13_{2\,11}$	$14_{3\,12}$
3063.54158	17.6	$5_{4\,2}$	$6_{5\,1}$
		$5_{4\,1}$	$6_{5\,2}$
3063.54055	25.0	$15_{2\,14}$	$16_{1\,15}$
3063.53708	36.2	$16_{0\,16}$	$17_{1\,17}$
		$16_{1\,16}$	$17_{0\,17}$
3063.51723	13.6	$14_{2\,12}$	$15_{3\,13}$
3063.49721	7.5	$8_{3\,5}$	$9_{4\,6}$
3063.49485	11.0	$15_{3\,13}$	$16_{2\,14}$
3063.47984	6.2	$16_{2\,15}$	$17_{1\,16}$
3063.47941	15.5	$16_{1\,15}$	$17_{2\,16}$
3063.47509	34.0	$17_{1\,17}$	$18_{0\,18}$
		$17_{0\,17}$	$18_{1\,18}$
3063.46988	29.8	$6_{4\,3}$	$7_{5\,2}$
		$6_{4\,2}$	$7_{5\,3}$
3063.46821	14.8	$15_{2\,13}$	$16_{3\,14}$
3063.41824	11.1	$17_{2\,16}$	$18_{1\,17}$
3063.41793	13.9	$17_{1\,16}$	$18_{2\,17}$
3063.41210	25.0	$16_{2\,14}$	$17_{3\,15}$
‡		$18_{0\,18}$	$19_{1\,19}$
‡		$18_{1\,18}$	$19_{0\,19}$
3063.40565	25.7	$5_{5\,0}$	$6_{6\,1}$
		$5_{5\,1}$	$6_{6\,0}$
3063.36585	14.9	$17_{3\,15}$	$18_{2\,16}$
‡3063.36301	24.8	$19_{0\,19}$	$20_{1\,20}$
‡		$19_{1\,19}$	$20_{0\,20}$
3063.35782	17.6	$18_{2\,17}$	$19_{1\,18}$
		$18_{1\,17}$	$19_{2\,18}$
3063.35753	13.4	$17_{2\,15}$	$18_{3\,16}$
3063.34885	7.7	$17_{4\,14}$	$18_{3\,15}$
‡3063.33609	21.6	$6_{5\,1}$	$7_{6\,2}$
‡		$6_{5\,2}$	$7_{6\,1}$
3063.32701	9.8	$8_{4\,5}$	$9_{5\,4}$
‡3063.30043	12.6	$18_{2\,16}$	$19_{3\,17}$
3063.29860	13.3	$18_{2\,16}$	$19_{3\,17}$
‡		$19_{1\,18}$	$20_{2\,19}$
‡		$19_{2\,18}$	$20_{1\,19}$
‡3065.29626	11.9	$20_{0\,20}$	$21_{1\,21}$
‡		$20_{1\,20}$	$21_{0\,21}$
3063.26565	4.3	$9_{4\,5}$	$10_{5\,6}$
‡3063.26440	17.7	$7_{5\,2}$	$8_{6\,3}$
‡		$7_{5\,3}$	$8_{6\,2}$
3063.25486	7.8	$9_{4\,6}$	$10_{5\,5}$
3063.23951	10.7	$19_{2\,17}$	$20_{3\,18}$
‡3063.23300	13.1	$20_{1\,19}$	$21_{2\,20}$
‡		$20_{2\,19}$	$21_{1\,20}$
3063.22921	10.8	$21_{0\,21}$	$22_{1\,22}$
		$21_{1\,21}$	$22_{0\,22}$
3063.20411	6.6	$10_{4\,6}$	$11_{5\,7}$
‡3063.20272	18.5	$6_{6\,0}$	$7_{7\,1}$
‡		$6_{6\,1}$	$7_{7\,0}$
‡3063.19296	13.6	$8_{5\,3}$	$9_{6\,4}$
‡		$8_{5\,4}$	$9_{6\,3}$
3063.18129	9.6	$10_{4\,7}$	$11_{5\,6}$
		$20_{3\,18}$	$21_{2\,19}$

‡3063.17017	8.5	22_{022}	23_{123}
‡		22_{122}	23_{023}
‡3063.13159	17.3	7_{61}	8_{72}
‡		7_{62}	8_{71}
3063.12171	3.0	9_{54}	10_{65}
3063.12137	9.0	9_{55}	10_{64}

3063.10608	9.9	23_{123}	24_{024}
		23_{023}	24_{124}
‡3063.06041	9.4	8_{62}	9_{73}
‡		8_{63}	9_{72}
3063.05082	4.3	23_{222}	24_{123}
		23_{122}	24_{223}
3063.04365	6.1	24_{024}	25_{125}
		24_{124}	25_{025}

Table VIII: The possible dark states for mode coupling observed in the pyrazine spectrum.

Energy (cm^{-1})	Components	Description of States
3066	$\nu_{14} + \nu_{20} + \nu_{23}$	Out-of-plane skeletal bend + C-C stretch + Out-of-plane C-H bend
3067	$\nu_3 + \nu_{11} + \nu_{22}$	C-H bend + C-H bend + Skeletal deformation
3067.14	$\nu_5 + 3\nu_7 + \nu_{12} + \nu_{24}$	Ring deformation + 3 Out-of-plane ring deformation + Ring deformation + Out-of-plane skeletal bend
3069.96	$2\nu_5 + \nu_{14} + \nu_{22} + \nu_{24}$	2 Ring deformation + Out-of-plane skeletal bend + Skeletal deformation + Out-of-plane skeletal bend
3070.56	$4\nu_7 + \nu_8 + \nu_{23}$	4 Out-of-plane ring deformation + Out-of-plane C-H bend + Out-of-plane C-H bend
3072.64	$\nu_{14} + \nu_{22} + \nu_{23} + 2\nu_{24}$	Out-of-plane skeletal bend + Skeletal deformation + Out-of-plane C-H bend + 2 Out-of-plane skeletal deformation
3074	$\nu_5 + \nu_{13} + \nu_{22} + \nu_{23}$	Ring deformation + Out-of-plane C-H bend + Skeletal deformation + Out-of-plane C-H bend